1-1-2005

Particle image velocimetry study of a skid steer loader cooling fan

John W. Laage
Iowa State University

Particle image velocimetry study of a skid steer loader cooling fan

by

John W. Laage

A thesis submitted to the graduate faculty

in partial fulfillment of the requirements for the degree of

MASTER OF SCIENCE

Major: Mechanical Engineering

Program of Study Committee:
M. G. Olsen, Co-major Professor
J. A. Mann III, Co-major Professor
T. I-Ping Shih

Iowa State University

Ames, Iowa

2005

Graduate College
Iowa State University

This is to certify that the master's thesis of

John W. Laage

has met the thesis requirements of Iowa State University

TABLE OF CONTENTS

LIST OF FIGURES

ACKNOWLEDGEMENTS

I would like to thank my co-major professors, Dr. Michael Olsen and Dr. Adin Mann for their patience, support, and advice during the writing of this thesis and the research that preceded it. Without their help this thesis would not have been possible.

Additionally I would like to thank the Bobcat Corporation and Brad Ellingson for funding this project and providing insight and direction.

I would also like to thank Pranay Mahendra, Dan Eiler, Paul Melzer, and Ashli Armstrong who provided invaluable assistance with the research work.

I would like to dedicate this thesis to my wife Ellen, who has provided unwavering support throughout the process which has culminated in this thesis.

ABSTRACT

Reducing noise generation in construction and farm machinery has become increasingly necessary to comply with stringent noise regulations. This need is particularly challenging in the design of skid steer loaders where machine space is tightly allocated, and the operator is close to the noise sources. In this thesis, particle image velocimetry (PIV) is used to study airflow in a skid steer loader's cooling package with an emphasis on gaining insights into strategies for noise reduction. The centrifugal fan used in this package is installed in a blower housing with two outlets and one inlet. PIV data were taken near the fan on both sides of the blower housing. Ensembles of images were collected both at specified fan positions and randomly to obtain an average of the flow. Sound experiments were also performed to ascertain the result of various conditions.

Experiments with the production fan and blower housing suggested that the system is operating under substantial restriction. Various strategies for investigating blower performance were investigated. These included a volute insert and fans with altered blade shapes and with impeller shrouds attached to the blades opposite the base plate. The volute consistently increased the sound produced when it was used due to the volute tongue interacting with the fan. Both fans with rings reduced noise production with the greatest reduction for the fan with the larger ring.

The effectiveness of the individual fan blades was studied by collecting data at twenty-seven evenly spaced fan positions over one revolution of the fan. The data suggested that the fan blades were performing similarly.

Finally, mean flow data were collected in the near-fan region of the blower housing without the volute cutoff and indicated reingestion of flow into the fan. A volute was produced based on the PIV data to prohibit this reingestion. The volute stopped the recirculation but caused increased noise and decreased flow.

INTRODUCTION

1.1 Skid Steer Loaders

Generically defined, a skid steer loader is a machine with four driven wheels which are controlled independently on either side of the machine for steering. A hydraulic loading arm equipped with a bucket, forks or other means of engaging a load is mounted at the front of the machine. Skid steer loaders were developed to meet the constraints of material handling in close quarters. Early models were designed to remove turkey manure from growing houses. These machines were required to pass through narrow doors, pick up several hundred pounds of payload, turn in their own length and deliver the load outside. Markets for these versatile machines developed wherever material handling power with maneuverability was needed, replacing manual labor.

The design constraints for these machines include the need for compactness, maneuverability, durability and operator comfort and convenience. A typical machine has hydraulic power transmission to the wheels as well as to the bucket. This arrangement has resulted in powerful machines with excellent maneuverability.

1.2 Background

Skid steer loader manufacturers are constantly challenged by the need to improve machine performance and convenience while also complying with changing regulatory requirements. One of the design constraints on skid steer loaders is the quantity of noise produced during operation. The compact design of the skid steer loader places the operator close to any noise that it produces. Also, regulatory limits are imposed on noise production. There are many sources of noise during skid steer loader operation, and the sound produced by air flowing through the cooling package is one of the major causes of machine noise.

Changes to improve machine performance often result in increased noise production. For example, as machine power is increased, heat rejection requirements are also increased. Thus, a larger engine requires additional cooling capacity. The hydraulic system must then also have increased cooling capacity. Air conditioning further adds to the cooling load. One significant design constraint in a skid steer loader is that cooling capacity must often be increased within the tightly allocated machine space. Increasing cooling capacity requires increasing the performance of the heat exchangers. This can be accomplished either by enlarging the heat exchangers or by moving air through the existing heat exchangers at a higher speed. Space constraints usually limit design changes to the second option. Since moving air through the cooling package at higher speed can usually be accomplished by increasing fan speed, this becomes a simply implemented, least cost solution. However this method results in increased noise production as a drawback.

1.3 Cooling package

The skid steer loader cooling package is positioned above the engine compartment and behind the operator. Air used for cooling enters behind the operator's location, point A, Fig. 1.1. Air is admitted to the cooling package through a perforated grill which excludes any airborne debris present. Air exits the cooling package through two symmetrically located outlets on either side of the machine, point B, Fig. 1.1.

Figure 1.1 Skid Steer Loader: (A) Cooling Air Inlet, (B) Cooling Air Exhaust

The cooling package includes three heat exchangers, a fan, and a blower housing. The heat exchangers are secured in the radiator assembly, Fig. 1.2, which is mated to the blower housing. A circular opening in the radiator assembly matches the blower housing inlet. The heat exchangers are mounted serially with an evaporator for air conditioning first. An oil cooler is next in order, and last is a radiator which serves the engine.

The cooling fan consists of 9 blades integral with a lower base plate and hub. Blade spacing is uneven to reduce harmonic acoustical effects. The blades leave an open center and slope toward the center of the base plate as the base plate is approached. A set of smaller blades is located on the opposite side of the fan base plate, Fig. 1.3. The base plate is located 15 mm above the blower housing floor when assembled.

The blower housing encircles the fan and guides used cooling air out of the cooling package. Air is drawn from the radiator assembly through a circular opening in the top of the

blower housing. A lesser airflow out of the engine compartment is maintained by the small blades on the underside of the fan base plate. The blower housing has two outlets located on opposite sides of the fan. Air is also discharged from the blower housing wall through small holes (1 inch diameter), as shown in Fig. 1.4, placed to provide spot cooling for machine components.

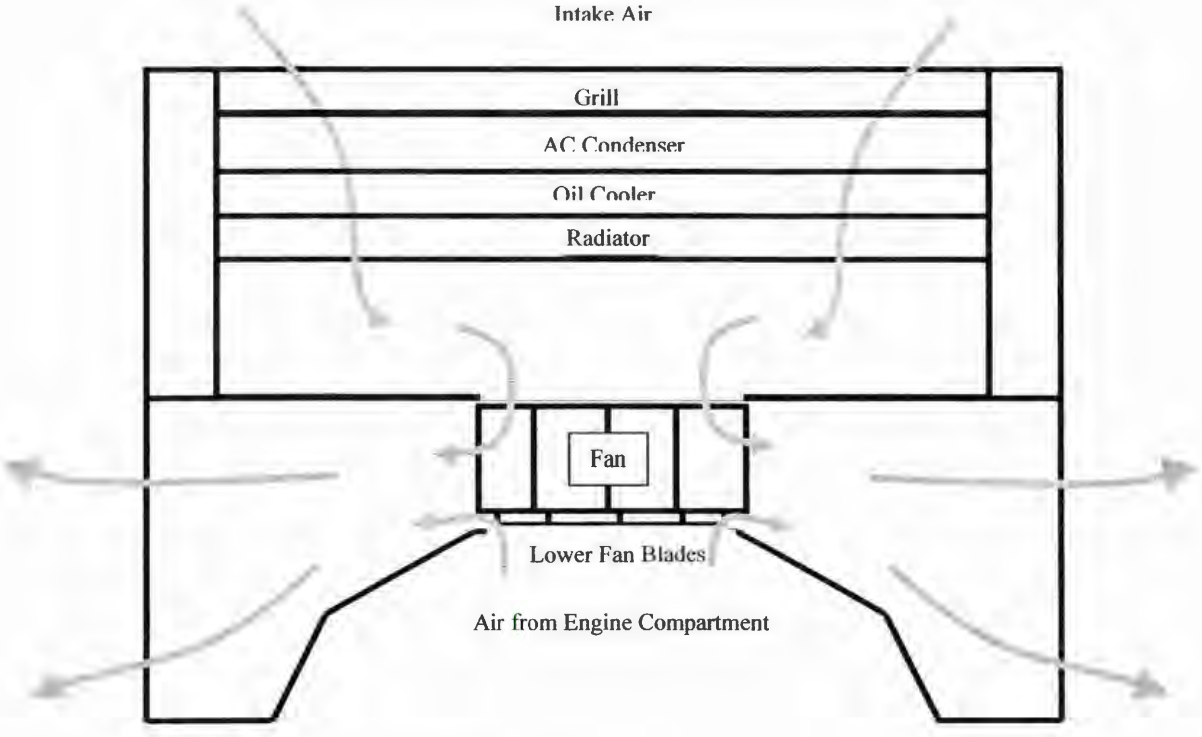

Figure 1.2 Schematic of Cooling Package

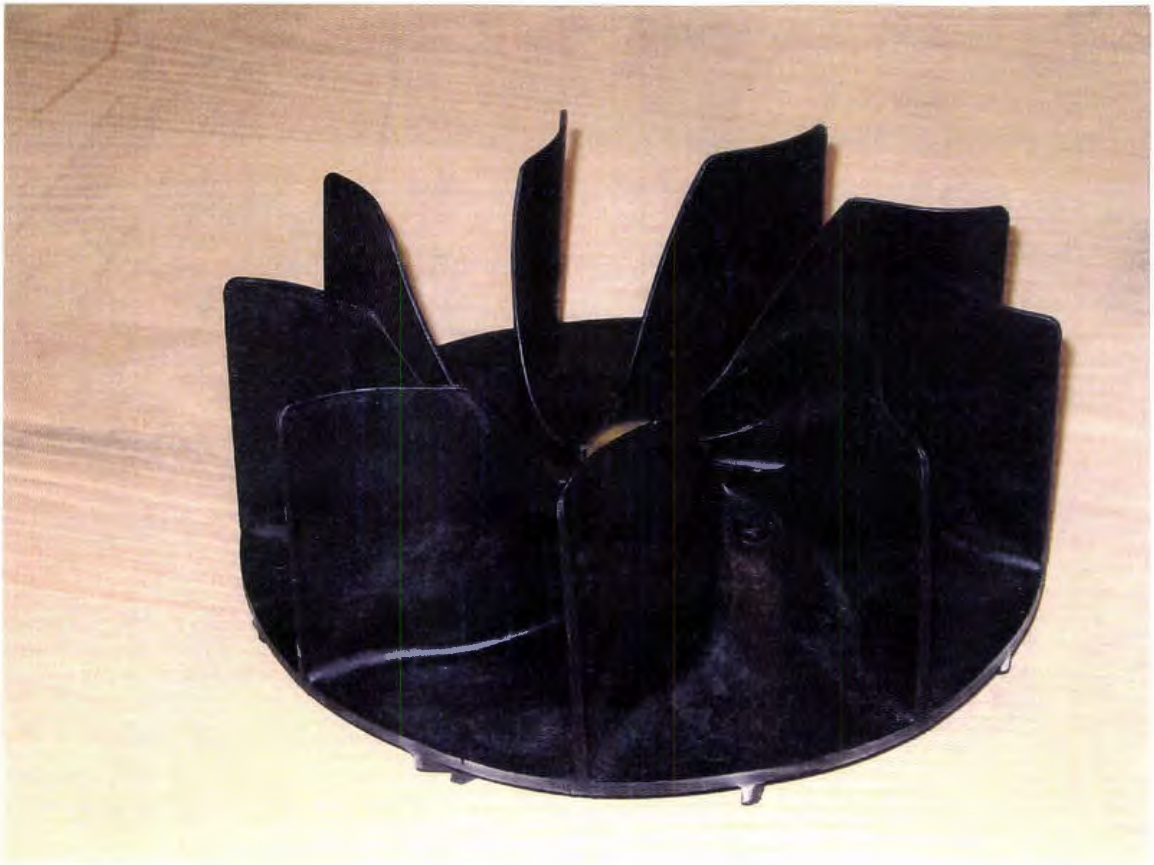

Figure 1.3 Fan

Figure 1.4 Spot Cooling Holes in Blower Housing (A)

1.4 Literature review

To the author's knowledge, the work presented here represents the first attempt to collect PIV data in a commercially produced blower housing assembly for a centrifugal fan. Because of their importance in so many applications, a number of previous experimental studies exist for both centrifugal and axial fan geometries using various experimental techniques, including hot wire anemometry, laser doppler velocimetry and particle image velocimetry. However, literature detailing the use of PIV in centrifugal fan studies is extremely limited. The following section is a brief summary of some of the existing literature for both axial flow and centrifugal fans, especially studies using PIV.

Fehse and Neise (1998) reported on an investigation of the mechanisms of low frequency (20-200 Hz) noise production in centrifugal fans. Their hypothesis was that this noise resulted from flow separation from the impeller and /or fan housing. Impellers with five different geometries were tested in the same fan housing. All impellers used a shroud or ring attached to the blades opposite the base plate. Two of the impellers were equipped with transducers to ascertain the pressure at various points on the impeller blades. Pressure was also measured at points in the fan housing walls. Hot wire anemometry was employed to measure the velocity distribution and turbulence intensity at the impeller exit. Fehse and Neise concluded that the design of the fan impeller was the most important factor in reducing low frequency noise production in centrifugal fans. The fan shroud or ring geometry is important in that a small radius of curvature leads to airflow separation with accompanying non-uniform flow and turbulence. Increasing the radius of curvature improves flow conditions, resulting in reduced noise generation.

Lee, Baek and Myung (2003) employed laser doppler velocimetry (LDV) to investigate the structure of tip leakage in a forward swept axial flow fan. LDV is a nonintrusive velocity measurement technique that provides three dimensional flowfield data, by measuring velocity at one point at a time. By traversing the LDV station through the flowfield, Lee, Baek and Myung obtained mean velocity data throughout the flowfield. The experimentally measured vectors were then compared to computational results to assess the validity of their computational model.

Hamkins and Flack (1987) reported results of LDV measurements in shrouded and un-shrouded radial flow pump impellers. The pump components were made from Plexiglas to facilitate optical access. Experimental results were used to calculate the pump's slip factor and to assist in development of computational models.

Yoon and Lee (2004) used stereoscopic PIV to measure the flowfield behind a forward swept five bladed axial-fan. They performed these measurements in a water tank to make flow seeding easier. Stereoscopic PIV is usually done using two cameras which capture seed particle images in the laser sheet from two different angles simultaneously. The information from both cameras allows calculation of the out of plane velocity component in addition to the two-dimensional velocity vector field. A periodic flow structure related to the phase angle of the blades was identified. This structure could be identified as the flow moved downstream. Counterclockwise vortices were shed from the blade tips, while clockwise vortices were found in the hub region.

Paone, Reithmuller, and Braembussche (1989) measured fluid velocities in a centrifugal pump's diffuser using PIV. As in the study of Hamkins and Flack, the pump's impeller and external housing were made of Plexiglas. The measured velocities were

compared to velocities measured by laser doppler velocimetry. This study showed that PIV could be useful in evaluation of flows found in turbomachinery.

As computers continue to improve in computational speed, computational fluid dynamics (CFD) has become a powerful tool in analysis of many turbulent flows, including fan flows. However, researchers often rely on experimental results to validate the predictions of CFD models. Velarde-Suarez *et al.* (2000) performed experimental and numerical studies of aerodynamic tonal noise generation in a centrifugal fan with backward curved blades. Emphasis was focused on impeller-volute interactions, particularly the effect of distance from the impeller to the volute tongue. The acoustic forcing term for computation was derived using experimental velocity data attributed to Shepherd and Lafontaine (1992) that was obtained using PIV. Suarez *et al.* state that the impeller/volute tongue interaction is the major source of pressure fluctuations which have a direct relationship to noise generation. The simulation that they employed indicated that tone noise increases when the distance between impeller and volute decreases. This was supported by their experimental sound power measurements.

Chu, Dong, and Katz (1995a) employed PIV measurements to calculate the phase averaged pressure field in a centrifugal pump. The original pump casing was replaced with a transparent one to allow optical access. Pressures computed from the velocity vector field were within 10% in most cases according to error analysis. It could also be shown that vorticity could not be neglected in a direction normal to a streamline. This indicates that the potential flow model cannot be used to describe the flow correctly.

In another paper Chu, Dong, and Katz (1995b) extended the work described above to analyze blade/tongue interactions. Maps of phase averaged pressure distributions were

calculated from the PIV velocity vector fields. Noise measurements were compared to pressure fluctuations. They concluded that since dominating phenomena appear to be connected to blade and tongue interactions, increasing the distance between the blade and tongue appears likely to reduce noise produced.

Meakhail *et al.* (2001, Parts I and II) used PIV to measure the instantaneous flowfield in a fan specifically built for PIV experiments. All parts of this centrifugal fan assembly were made from Plexiglas to facilitate optical access for the PIV measurements. They reported results for the fan equipped with both a vaneless (Part I) and vaned diffuser (Part II). Meakhail *et al.* concluded that:

- Flow into the diffuser, either vaned or vaneless is mainly influenced by flow exiting the impeller
- Flow separation from the suction side of the fan blades should be avoided
- Flow at the impeller discharge is affected by inlet geometry
- Additional studies were needed to adapt different vaned diffuser geometries to varying flows
- The flowfield is quite different for different flow rates

Meakhail and Park (2005) studied the same centrifugal fan using CFD and compared the results to the PIV experimental measurements previously obtained (Meakhail *et al.* 2001, Parts I and II). The impeller was configured similarly to the fan used in the work for this thesis, and thus this study is of particular importance to the work presented here. Impeller blades were fastened to a circular base plate. Air entered from the side opposite the base plate and left the impeller through the diffuser. The diffuser was built in two different

versions, with and without vanes. Air leaving the diffuser entered a volute which guided the air to a discharge port.

While this fan system had some differences from that used in experiments for this thesis, the similarities in the geometry of the two fan/impellers make the work of Meakhail and Park important for comparison. Both systems admit air in an open center on the side of the fan opposite the hub. Meakhail and Park have published calculated vector fields for their test fan operating at 40%, 100% and 150% of design capacity. The images for these operating conditions show higher velocity air near the base of the fan/impeller. The velocity variation across the fan blades becomes less pronounced as the fan operating load is increased. The vector fields obtained with the system operating at 150% of capacity show a near constant velocity across the depth of the fan. As will be seen later, the vector fields for the fan studied for this thesis generally show a considerable variation in air velocity from the base of the fan to its top. This supports the hypothesis that the fan output is severely restricted by inlet conditions.

The work undertaken for this thesis is unique in that a centrifugal fan system used in a production machine was the subject of PIV analysis. The existing fan system was modified for optical access, and PIV measurements were performed to discover the flow characteristics of this system. Additionally the fan and blower housing system employed a unique dual opposed outlet design which was also investigated as a part of this work

1.5 Objective

Improving the blower design requires a greater understanding of the flow phenomena that represent mechanisms of noise production and flow inefficiency in a skid steer loaders cooling package. In this thesis, particle image velocimetry is used to study the air flow through a skid steer loaders cooling package with the objective of identifying sources of noise production and flow inefficiency.

2 EXPERIMENTAL APPARATUS

2.1 Particle Image Velocimetry System

Flow within the blower housing was studied using particle image velocimetry (PIV). PIV has an advantage over more "traditional" velocity measurement techniques, such as hot-wires and Pitot-static probes, in that it is a non-intrusive technique. PIV is optically based and provides instantaneous velocity field data within a selected plane of the flowfield. The whole field velocity data is captured, allowing visualization of flow structures at a given moment. Ensembles of individual velocity field realizations can then be averaged to yield mean flowfield data within the measurement plane.

Figure 2.1 shows the schematic layout of a PIV system.

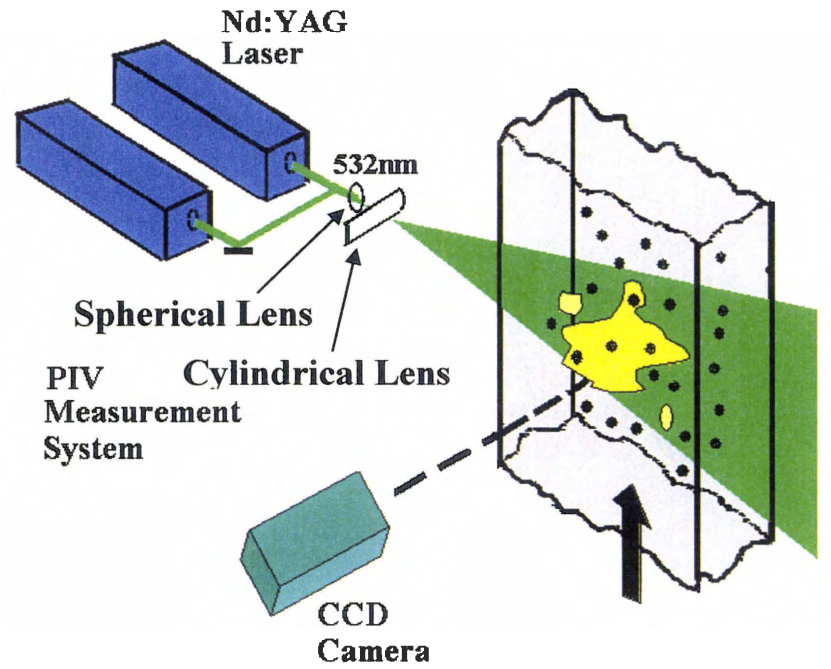

Figure 2.1 Schematic of PIV System

In a typical PIV experiment, two pulses of laser light are projected as a planar sheet to illuminate an area of the flow at two instants in time microseconds apart, essentially acting as a high powered strobe light. Particles introduced into the flow scatter light when illuminated, and images of the particles are recorded by a CCD camera. The images are then analyzed using a cross-correlation technique to obtain a vector representation of velocities within the flow field.

The light scattering particles used in this study were 1 micron diameter droplets of olive oil that were produced by a LaVision VZ seeder atomizer. Other seed materials, such as silicone oil, could also be used, but olive oil was chosen for this particular experiment since it is inexpensive and non-toxic. However, since the olive oil is organic, the seeder must be periodically cleaned to remove any decomposing olive oil droplet residue. If left unremoved, the residual olive oil both degrades the performance of the seeder and also leads to foul stench in the laboratory.

Laser lighting for the PIV experiments was provided by a New Wave Research, model Gemini 15, Nd:YAG laser. The PIV laser consists of two individual lasers combined into a single system. The light emitted by the two laser heads is combined within the laser body and with careful alignment exit the laser along identical paths. The two laser heads within this unit are capable of generating a pair of light pulses separated by as small of a time interval as is necessitated by experimental conditions. The energy per pulse is adjustable up to a maximum of 120 mJ per pulse. The maximum cycling rate is 15 Hz. In the current experiments, the laser power was set close to the maximum in order to provide adequate illumination over the fields of view of the camera.

The laser was mounted on a Newport optical table, providing a solid base for the laser system that was free from mechanical vibrations. An optical rail was attached to the table, and this optical rail was used to mount the cylindrical and spherical lenses needed to produce the PIV light sheet. Spherical lenses with focal lengths of .25, .5 and 1 meter were combined with cylindrical lenses with focal lengths of -12.7 and -25.4 to produce the laser light sheet. A high-energy mirror was used to deflect light into the vertical direction for experimental setups in which the light sheet was introduced through one of the lower windows which had been installed in the blower housing. Figure 2.2 shows the PIV system and the test stand used for this work set up for viewing flow in a vertical plane in the right hand outlet of the cooling package.

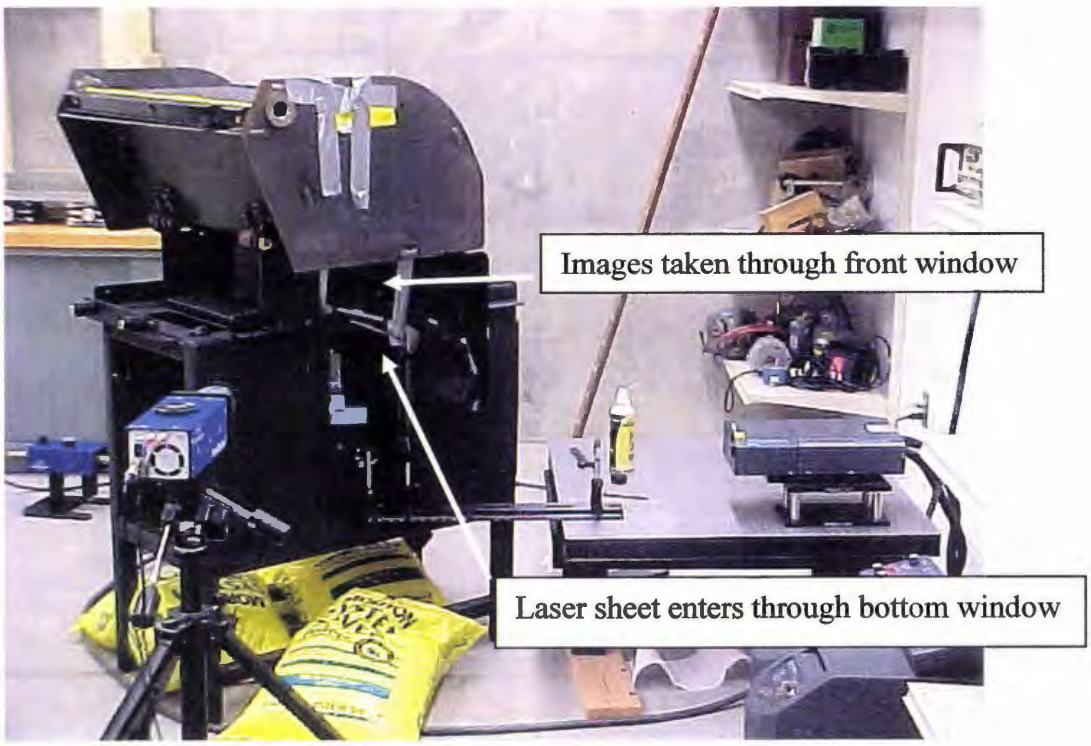

Figure 2.2 Photograph of PIV System with Test Stand

The optimal thickness for the laser light sheet used for PIV is influenced by the magnitude of flow velocity out of the plane of the laser sheet and the seeding density. Ideally, the laser sheet thickness should be made as small as possible so that the measured velocity field represents a two-dimensional snapshot of the flowfield. However, practical considerations, such as seeding limitations and out-of-plane fluid motion, often make it necessary to use a thicker light sheet in a given experiment. Low particle seeding density and particles exiting the light sheet reduce the number of particles available for PIV analysis, and a thicker light sheet must be used to increase the number of seed particles within each measurement volume. Similarly, when significant out of plane velocity is present, the use of a thicker light sheet is a necessary compromise in order to make sure that the out-of-plane particle motion does not cause the particles to leave the location of the light sheets between laser pulses. In the present work, a laser sheet thickness of 2 mm was found to provide good results with the conditions encountered in the flow studied here.

Flowfield imaging was performed using a LaVision Flowmaster 3S CCD camera. The CCD sensor for this camera has a pixel size of 6.7 x 6.7 μm and measures 1280 by 1024 pixels. This is a fast frame rate interline frame transfer camera capable of taking 8 pictures per second or 4 paired images, resulting in a PIV data collection rate of 4 Hz. The camera was fitted with a Sigma AF-MF 28-105 mm f3.8 zoom lens. The use of a zoom lens allowed flexibility when positioning the camera since the viewing field could be adjusted to match the cameras imaging CCD at variable distances from the flowfield.

Distance on the images was calibrated by photographing a ruler with millimeter markings positioned in the plane of the laser light sheet. Then a known distance in the image

could be set in the analysis software, allowing distance and velocity measurements in the vector images to be produced.

The lasers and camera were controlled by a computer running LaVision Davis software version 6.2.3. The computer also contained proprietary PCI computer cards for system synchronization and digital frame grabbing, also from LaVision. PIV data could be collected in triggered mode, synchronized to the fan shaft position or continuously (that is, untriggered with fan shaft position). The system recorded the raw PIV images on a hard drive for later analysis. After the PIV images were collected and stored, they were processed to yield velocity field data, also by the Davis software.

2.2 Test Stand

Because logistical and experimental constraints make it impossible to perform experiments on an actual skid steer loader in the laboratory, a test stand was constructed on which the skid steer loader cooling package was mounted and operated. This test stand allowed testing to take place in available laboratory facilities. The test stand was designed such that it was easily modified, making possible the use of a wide array of experimental flow and noise measurement techniques. The skid steer loader test stand used in the current study was not designed and built at Iowa State University. Instead the skid steer loader manufacturer provided a test stand that had been used at their facility for this testing and allowed researchers at ISU to modify the test stand as necessary to make the planned experiments possible. The test stand assembly is shown in Fig. 2.3.

Figure 2.3 Test Stand

The main purpose of the test stand was to provide a firm, steady mounting for the blower housing and radiator assembly that make up the skid steer loader cooling package. In order to provide a solid base, the test stand "skeleton" consisted of a rectangular frame made from 2"x 2" steel tubing. The sides of the test stand were enclosed by 1/8 inch steel sheet. The production mounting for the blower system was then welded onto the top of the test stand and the fan and blower housing were bolted onto the production mounting.

The blower fan drive was modified from the production 90 degree gear drive to a straight through drive. The blower fan drive assembly is shown in Fig. 2.4.

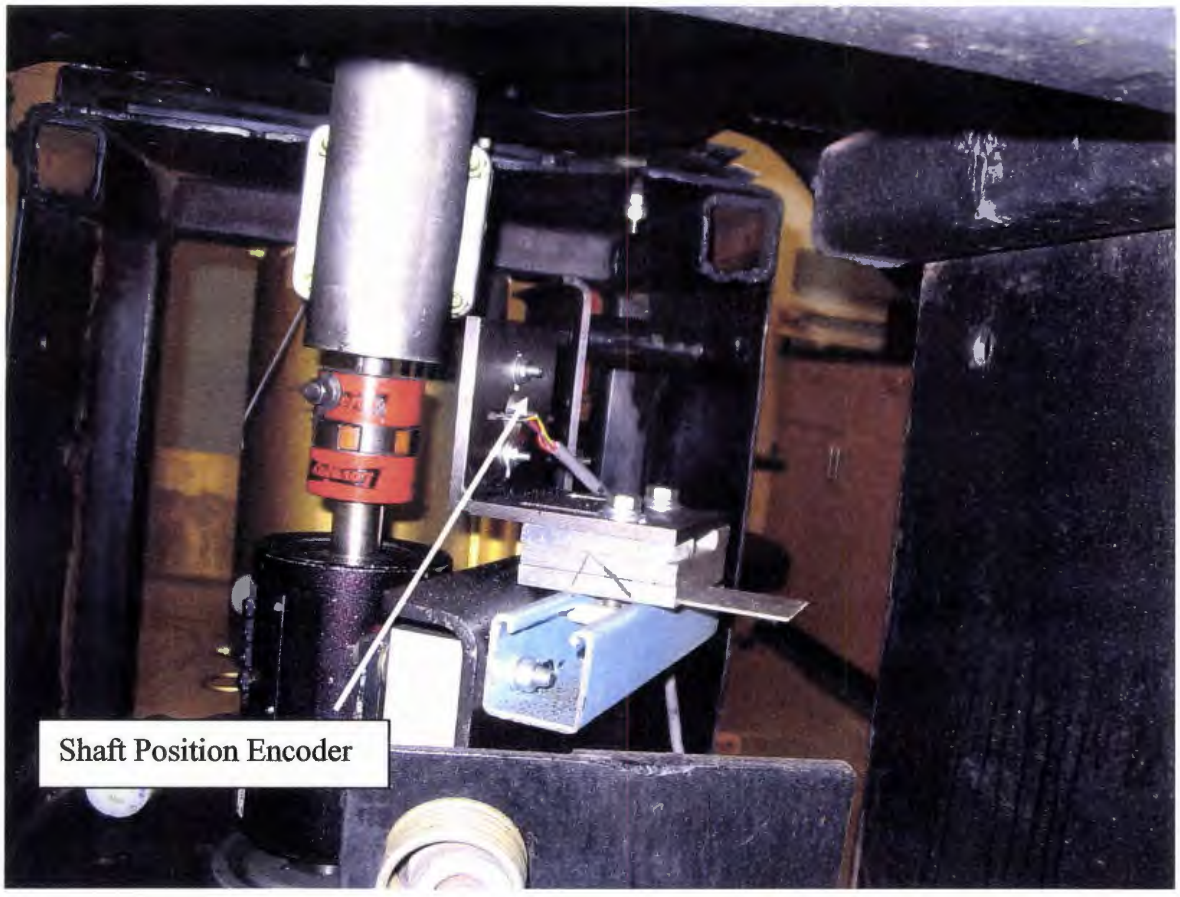

Figure 2.4 Modified Fan Drive

A LeBow 1401 torque sensor was included in the fan drive to allow the power to be measured during operation. However, this sensor was not used during the experiments described here. The shaft was initially driven by a Dayton Model 3N339C 5 hp 3 phase electric motor using a v-belt. The early testing was done using the 5 hp Dayton electric motor. This included all the PIV work presented in this thesis. Later, during flow testing which required longer run times, it was found that the 5 hp motor was unable to maintain 3200 rpm at the fan shaft. The 5 hp motor was then replaced by a 7.5 hp Baldor EM 3219 T motor for the remaining experiments. This larger motor allowed the required fan shaft speed to be maintained indefinitely. Fan shaft speed was controlled by varying the motor speed

with a Baldor 1D15V210-ER variable frequency motor controller. Among the outputs of the Baldor motor controller were voltage and current information, allowing power use to be determined.

During operation the test stand tended to vibrate and "walk" across the floor. This problem was solved by placing 80 lb bags of water softener salt upon the test stand to anchor it and dampen vibrations.

2.2.1 Modifications to the Test Stand for PIV Experiments

Particle image velocimetry (PIV) is an optically based experimental technique in which a laser sheet is used for illumination. Thus, the test stand had to be modified such that optical access could be provided both for the illuminating light sheet and also the imaging optics. To accomplish this, the mounting area for the blower housing onto the test stand was cut away on both sides underneath the discharge areas of the blower housing. Figure 2.5 shows the modified areas of the test stand. The robust construction of the test stand allowed this modification. Despite the rather large amount of material removed during this process, no indications were found during testing that the necessary structural integrity was violated by this change.

After cutting out the openings for optical access, the test stand was cleaned to prevent damage to the PIV equipment by loose debris. The stand was then painted black to reduce the potential for stray reflections which could both interfere with PIV and cause potential eye injury.

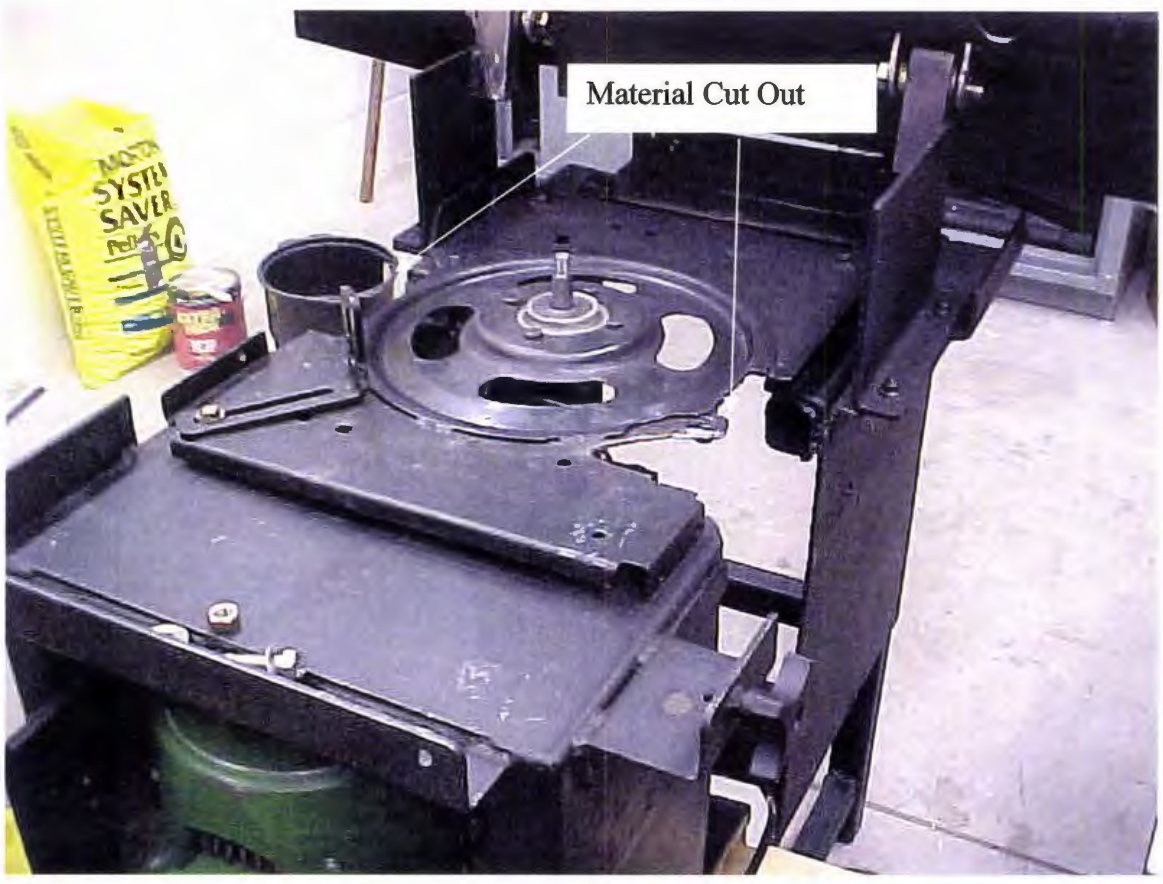

Figure 2.5 Material Cut Out From Test Stand for Optical Access

A shaft position encoder was added to facilitate taking multiple PIV images synchronized to a certain fan position and for measuring fan shaft rotation rate, Fig. 2.4. A VTL 13 D7-20 transmissive optoswitch made by Perkin Elmer Optoelectronics was chosen for the shaft encoder. This device incorporates an optical emitter and detector, separated by a small gap, in one package. The transmissive optoswitch was connected as shown in Fig. 2.6. A 5 volt signal is produced when the light path between the emitter and detector is interrupted.

The transmissive optoswitch was mounted adjacent to the fan shaft. A thin wire was attached to the fan shaft so that it passed between the emitter and detector as the shaft revolved producing one 5 V pulse per turn.

Since the signal occurs at the same point during each revolution, the signal was used to synchronize the PIV system to the fan. A delay time specified in the PIV software allowed the system to be triggered to only collect data when the shaft and fan blade were at a desired position. The time delay was varied to acquire data at different fan positions.

The signal was also received by a Labview program which output the shaft rpm.

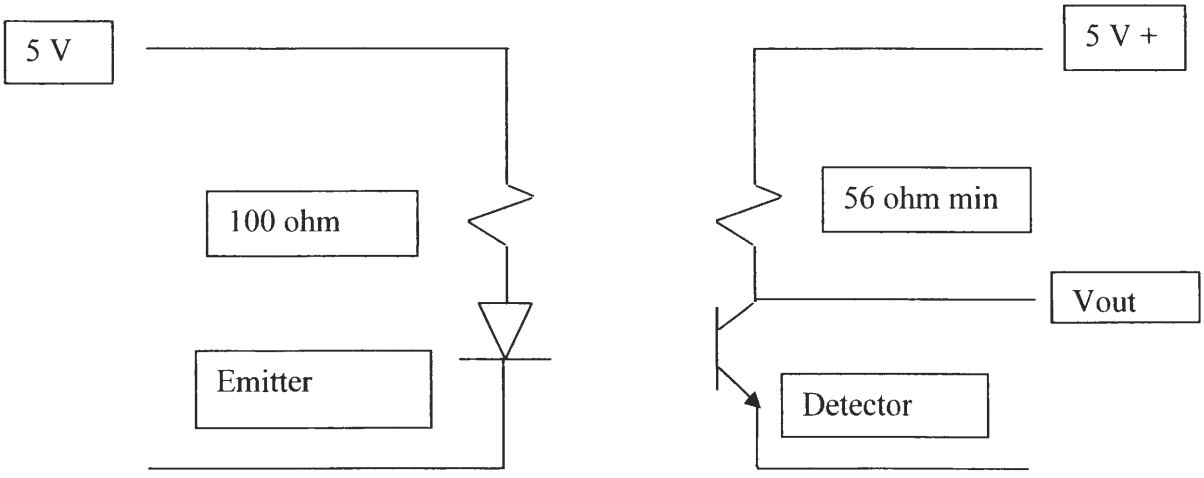

Figure 2.6 Circuit Diagram of the Shaft Encoder

2.2.2 Optical Access

PIV requires optical access to the region under study. A light sheet produced by the laser/lens system must be placed within the flow to illuminate the area of interest. Tracer particles within the light sheet must then be photographed for PIV analysis. PIV imaging is best done normal to the light sheet, thus optical access must be available from two directions oriented at 90 degrees to each other.

There are four surfaces on the blower housing which could have been chosen for optical access. The top surface marked A in Fig. 2.7 was flat over the whole outlet but was not used because the radiator assembly is installed immediately adjacent to this surface, prohibiting optical access through this surface. Extensive changes to the test setup would have been needed to use this area for optical access (although it would have been an ideal location). The rear vertical surface of the blower housing was not used for optical access because it is partly obscured by mounting hardware on the test stand. Also this area would see installation of experimental volute cutoffs on the left hand side which would cover the window.

Two areas of the blower housing were studied using PIV. These areas were located on either side of the fan focused on the "cutoff" region where air is separated from the fan. The areas studied were just beyond the fan and were 80 mm in width on the right side and 250 mm on the left. Optical access to the blower housing was obtained through two windows for each of these areas Fig. 2.8 on each side of the fan, one on the bottom of the housing and one through the vertical face of the housing.

Distortion of the light entering and leaving the flow area will impact the results of PIV analysis, and changes to the configuration of the blower housing will distort the flow

being studied. Initial PIV work was done with Plexiglas windows constructed to have no impact on the flow with contours that matched the blower housing geometry as closely as possible.

The blower housing is molded from polyethylene approximately 1/8 inch in thickness. This relatively thin plastic part limited options for securing transparent windows. Access to areas where the blower housing was flat was provided by cutting out the original material and fitting ¼ inch Plexiglas into the opening. The window was secured flush with the inside of the blower housing by gluing strips of Plexiglas to the window's edge where the 1/4 inch window material protruded above the 1/8 inch blower housing material. The window assembly was then fastened in place using duct tape. Any irregularities in the window's fit were filled and smoothed with modeling clay. Use of duct tape for fastening the windows eliminated fasteners which would protrude into the blower housing and disturb flow.

Areas with simple curvature were fitted with windows by bending the Plexiglas to match contours of the blower housing. Bending was accomplished by heating the plastic using an electric forced air heat gun. The heat-softened Plexiglas could then be bent. These windows were made from a 0.10 inch thick Plexiglas material which could be bent more readily than ¼ inch material. Since the thinner material was not available for fastening above the blower housing material narrow strips of Plexiglas were glued around the edges of these windows increasing thickness of the window. Plexiglas strips could then be glued to the edge thus produced and again duct tape was employed to secure the assembly.

The horizontal window marked A in Fig. 2.8 was bent to match the blower housing at a point where this could be done with no compound curvature. The curvature of this window

was acceptable for introducing the laser light sheet since the orientation of the curvature served only to augment the spreading of the light sheet begun by the lens system. Since PIV analysis was desired in both vertical and horizontal orientations, this window was also used for photographing a horizontal light sheet introduced through the vertical window. The images obtained in this manner were useful in the flat areas of the window but distorted in the area of the curvature.

Figure 2.7 Blower Housing: A indicates the flat surface referenced in the text

Figure 2.8 Blower Housing Showing Windows Installed on Left Side

The horizontal window installed for initial PIV did not allow access near the sidewalls of the blower housing and caused image distortion where it curved to match the configuration of the blower housing. Another blower housing was modified to incorporate a window which would avoid these difficulties with minimal change to the original blower housing configuration. A flat window, point A, in Fig. 2.9, was installed and the expansion of the original blower housing was delayed to a point just past this window.

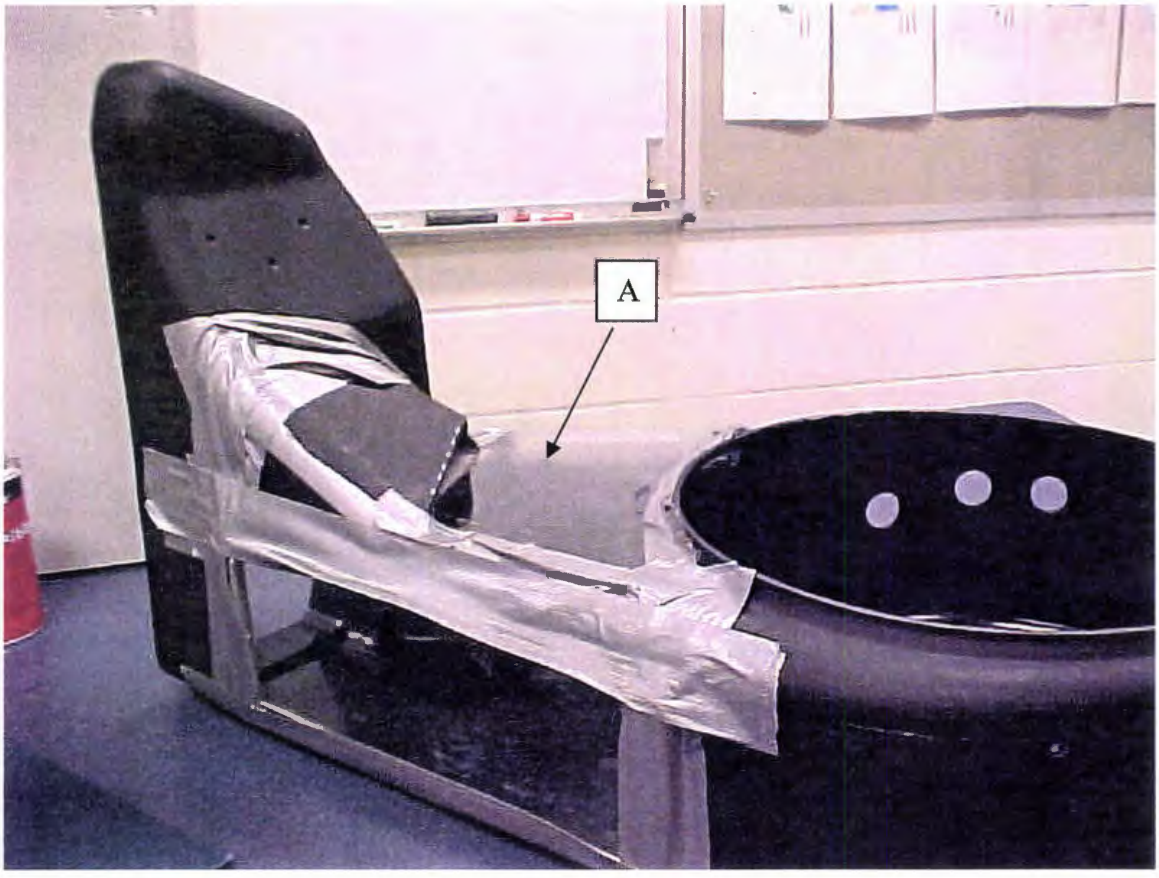

Figure 2.9 Blower Housing with Flat Horizontal Window

3 OBTAINING PIV DATA

As has been previously mentioned, to the author's knowledge the work presented here represents the first attempt to acquire PIV data in a centrifugal fan blower housing production assembly. As such, several difficulties associated with this flow geometry had to be overcome for the successful collection of PIV data. The following chapter describes the methodologies used to collect the PIV data, including such topics as the determination of the proper operating parameters and choice of experimental setup.

3.1. PIV Parameters for the Blower Housing Study

3.1.1 Seeding

Seeding is perhaps the most critical aspect of a successful PIV experiment. Obtaining the optimal seeding is a delicate balance between using enough seed so that there are enough particles for successful velocity vector determination and yet not using so much seed that either the test section becomes fouled from excess seed or that PIV images degrade to a useless speckle pattern. The seeding must also be introduced into the flowfield as uniformly as possible, since velocity vector data cannot be obtained in flowfield regions that contain little or no seed particles.

In the blower housing experiments, the quantity of olive oil seeding droplets introduced into the airflow for PIV was controlled by adjusting the air pressure supplied to the atomizer and by cycling the atomizer on and off. One important feature of the seeding strategy is that the PIV experiments were performed in an enclosed area. It was found that this was the best strategy for ensuring homogeneous seed distribution. The oil droplets were introduced into the room and mixed with the room air by the turbulence resulting from the

test air handling systems outlets. This produced a homogeneous mixture of air and olive oil droplets throughout the entire room which was then recirculated through the test system. Since the test room was well ventilated, seed was constantly depleted through the exhaust duct from the room. Therefore, to maintain as constant of a seed density as possible, it was necessary to replenish the seed in the room during experiments. Although it was found that successful PIV interrogation was possible over a range of seeding densities, it was advantageous to strive for the minimum density of PIV seeding needed, since increased seeding also increased the rate at which olive oil was deposited on the optical access windows. The PIV seeding density employed for this thesis was determined by experimenting with the seeder settings and operation and observing the quality of the resulting PIV vector fields.

The following seeding methodology was found to yield satisfactory results. First, the seeder was run for 30 seconds prior to the beginning of data collection to fill the room with sufficient seeding. The seeder was then turned off temporarily while data collection began. Then, to replenish the seed lost through the exhaust duct, the seeder was periodically turned on and off. The seeder would be turned on for 30 seconds, and then turned off for 30 seconds, and this process was repeated until the end of a particular run.

3.1.2 Laser Light Sheet

Another critical parameter for a PIV experiment is the geometry of the laser light sheet. Since only particles illuminated by the laser will appear in the PIV images, the laser light sheet determines the flowfield data collection region. The area covered by the light sheet is controlled by the focal length of the cylindrical lens and the distance the light travels

after it leaves the lens. The thickness of the laser light sheet is determined by the focal length of the spherical lens and the distance traveled from the lens to the flowfield. At the focus of the spherical lens the light sheet thickness is a minimum. Even at the focal point, the thickness of the light sheet remains finite due to diffraction effects. The light sheet thickness increases from the focal point at a rate determined by the focal length of the spherical lens. The farther the focal point is from the flowfield the thicker the light sheet will be. Usually, the light sheet thickness is minimized in the imaged region since that would yield the greatest possible spatial resolution in the out of plane direction. However, in some instances a thicker light sheet must be used due to either low seeding density or significant out of plane motion. In cases of low seed density, using a thicker light sheet will cause more particles to appear within each PIV image, making successful interrogation of the images more likely.

Out of plane motion will cause particles to leave the light sheet between the two laser pulses, and result in unsuccessful interrogation, and using a thicker light sheet in this situation will reduce the number of particles leaving the light sheet between laser pulses. In the present experiment, seed density was not a problem, but the highly three-dimensional nature of the flowfield resulted in a great deal of out of plane motion of seed particles. For this reason, the light sheet thickness in the current experiments was set to be 2 mm.

Of less critical importance than the spherical lens to successful PIV interrogation is the cylindrical lens that controls the spreading of the laser beam and the subsequent formation of the laser sheet. It is rather easy to find a cylindrical lens focal length and placement to adequately illuminate the flowfield. However, care must be taken in the placement of the cylindrical lens because allowing the focus of the spherical lens to coincide with the cylindrical lens can cause damage to the cylindrical lens due to concentration of

light energy. An assortment of cylindrical lens focal lengths and placements were used for the various measurement contained within this thesis.

3.1.3 Dt (delay time)

A general rule of thumb for designing PIV experiments is that the time delay between the two illuminating laser pulses (Δt) should be such that the particles move approximately $1/4^{th}$ the width of the interrogation window, also referred to as an interrogation spot, between the two laser pulses. This rule of thumb is a balance between two competing factors. First, PIV measurement error is inversely proportional to the distance moved by the seed particles, thus measurement error is minimized by making Δt as long as possible. However, if Δt is made too long, then seed particles will move out of the interrogation window between laser pulses, resulting in unsuccessful interrogation. Allowing the particles to move $1/4^{th}$ the width of the interrogation window has been found to be the optimum laser delay setting based on these factors.

In the present experiments, the interrogation window size is 32 pixels by 32 pixels, so ideally, the particles should move 8 pixels between laser pulses. However, even with the thick laser sheet that was used, there was too much out of plane motion in some regions of the flowfield to use a long enough Δt to achieve this large of a particle displacement. Instead, a Δt of 20 microseconds was used, corresponding to a particle displacement of approximately 5 pixels, or approximately $1/6^{th}$ of an interrogation spot.

The measurement error in PIV experiments is determined by the accuracy to which the signal peak location in the cross-correlation analysis can be determined (Prasad *et al* 1992). A conservative estimate for the accuracy of this determination is ±0.2 pixels. Since

the typical particle displacement in the set of measurements presented here is 5 pixels, measurement uncertainty can therefore be estimated to be ±4%. Note that this methodology for PIV error estimation tends to be *very* conservative, and recent results in other experiments at Iowa State University (Feng *et al.*, 2005) suggest that the actual experimental error is less than half of this value.

3.2 PIV Processing

3.2.1 Processing

The raw PIV images were divided into small regions, termed "interrogation spots" and interrogated to yield a velocity vector at each interrogation spot. The velocity vectors for each interrogation spot within the image constitute the instantaneous velocity vector field. A 32 by 32 pixel interrogation spot size was used for the work presented here. Successive spots were overlapped by 50% to increase the spatial resolution of the resulting velocity fields. In any PIV interrogation, there will always be some interrogation spots that yield spurious, or bad, velocity measurements. The number of these spurious vectors was reduced by restricting the search for correlated light intensity peaks to a window around the expected x- and y- velocities, Vx and Vy, such that the velocity search was limited to a box ± 5 pixels from the expected velocity vector, (Vx, Vy) within the interrogation spot. The number of spurious vectors was further reduced by comparing each measured velocity vector with the values of neighboring vectors and eliminating those that differed from the median value of their neighbors by too large of an amount. The median filter provided in the software was set to remove and replace vectors greater than 1.3 times the root mean square value of

neighboring vectors. The allowable range of vectors was restricted when needed to eliminate unreasonable values

The removal of spurious vectors results in empty spaces within the measured velocity vector fields. To eliminate these holes, missing vectors were replaced by interpolating using the velocities of valid neighboring vectors. Finally, high frequency noise in the measured velocity fields was eliminated by using a Gaussian smoothing algorithm provided in the LaVision software. The end results of the interrogation and post processing were velocity vector fields which were representative of the region examined without voids due to missing data.

3.2.2 Number of Images

The number of observations needed for analysis of a particular flow event depends on the type of analysis planned as well as the goals of that analysis. Reliable mean velocity field data can be obtained with a few hundred images. To demonstrate this, consider the results shown in Fig. 3.1, which is a surface plot that shows how averaged observations converged toward the average of 1000 observations as the number of observations averaged was increased. Figure 3.1 was made by producing a series of averaged velocity fields using ensembles of 100, 200, 300, etc., up to 1000 individual vector field realizations, all triggered at the same position of the fan shaft. An arbitrary horizontal coordinate in the averaged vector fields was selected and used to construct x-component of velocity profiles. Then the percentage changes with reference to the velocity value from the velocity field of 1000 averages were plotted (it was assumed *a priori* that an ensemble of 1000 velocity field realizations would yield a stable mean). Percentage change remained within 5 percent of the value for 1000 realization averages after only 200 velocity fields were averaged. Note that

statistical analysis of the flow to determine higher order statistical quantities, such as Reynolds stresses and turbulent kinetic energy requires a much large ensemble size. Reliable higher order statistics are obtained in data sets consisting of at least 1000 - 2000 or more observations, M. G. Olsen (2005).

PIV observations can consume considerable time for the computer to process the image files, and the stored PIV images and vector fields can also occupy large amounts of data storage media. For example, a typical processing time for 1000 PIV image sets is 1 hour. The PIV images and vector fields will occupy approximately 2 gigabytes of data storage space. However, once the time and money required to establish a successful PIV

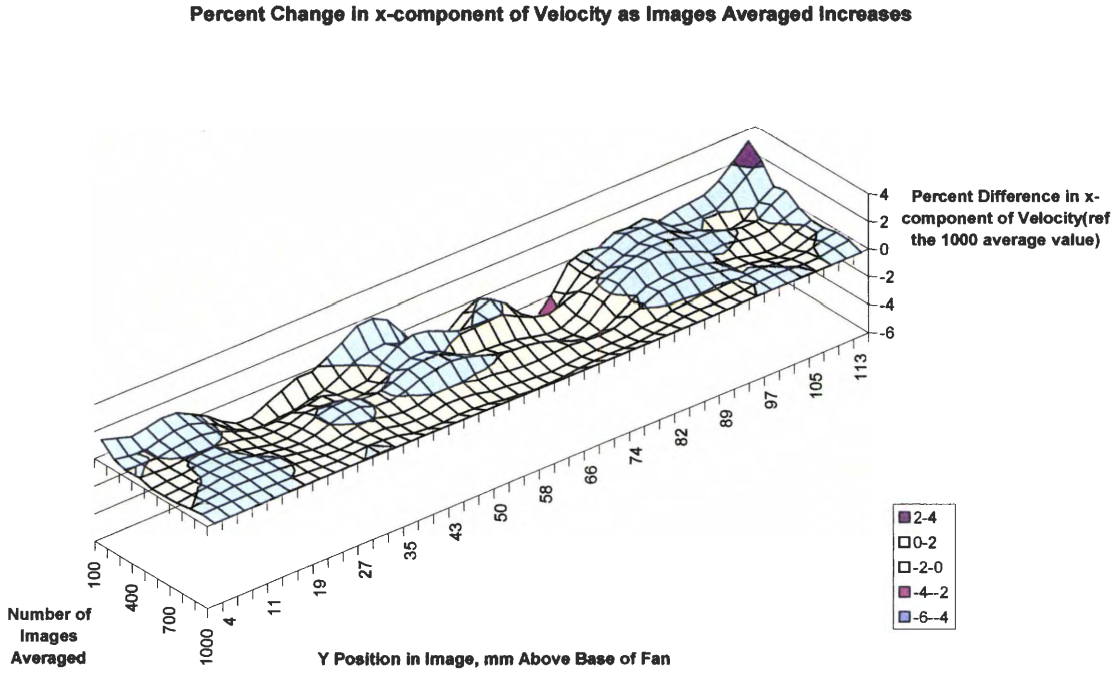

Figure 3.1 Change as Number of Observations Averaged Increases

setup and data storage strategy has been expended, large amounts of data can be accumulated in a short time with little additional expense. The cost of storage media as well as computer speed has changed significantly in a beneficial way during the time that work for this thesis

was performed. Thus the number of observations taken must be considered in light of the current circumstances

3.3 Elimination of Stray Light Sources

Ideally, the only light reaching the camera in a PIV experiment should be the light scattered from the seed particles, since it is only the seed particles that contain information about the velocity field. Light from other sources, such as stray room and reflected or scattered light from solid surfaces can lead to either difficulty in imaging the seed particles or erroneous velocity vector measurements that represent the velocities of the solid surfaces and not the moving fluid. Therefore, successful implementation of PIV requires careful control of the lighting in an experiment, both from the surroundings and the PIV system.

Ambient background light was eliminated by installing the test stand in a room which could be nearly completely closed off to outside light sources. The test stand and PIV equipment were controlled from outside the room, thus eliminating any interference due to stray light from light sources needed by the system operator. Only one small window to the room provided a path for light to enter the testing room, and the small amount of light that entered the testing room through this window was inconsequential.

Reflections and scattering from solid surfaces must also be minimized, because in the PIV system, light is only useful while confined to the light sheet which is passed through the region under study. The first step in the optical setup of the PIV laser and optics is to avoid light being reflected or redirected before entering the test section. In addition to making successful PIV measurements more difficult, stray light outside the test region can endanger personnel and optical equipment. The camera is especially susceptible to damage from stray light, as a laser beam reflected onto the CCD sensor array can cause permanent damage. The

light sheet is at its most powerful before entering the test section, and it is at this point that stray reflections or scattering are the most dangerous.

Even after the light sheet has passed through the plane which is being photographed for PIV analysis, reflections or scattering can become a potential problem. If the light sheet is reflected back across the region studied and out of the intended imaging plane, light scattered from seed outside the measurement plane could be included in the PIV images being collected resulting in an undesirable impact on results. A diffuse reflection can also cause problems since it tends to increase the background light level in a PIV image, making it difficult for light scattered from seed particles to be identified over this diffuse background glow. An example of the effect of a diffuse reflection from a solid surface can be seen in Fig. 3.2. In this Figure, the diffuse reflection off the surface of the volute insert results in a "flare" of light which obliterates nearby data. While it is seldom possible to completely eliminate stray light due to reflection or scattering from solid surfaces, attempts should be made to minimize it.

Reflection interference can be controlled by choice of the experimental setup. As an example, the reflection shown in Fig. 3.2 was later eliminated by aligning the light sheet so that it closely approached the edge of the insert without touching it.

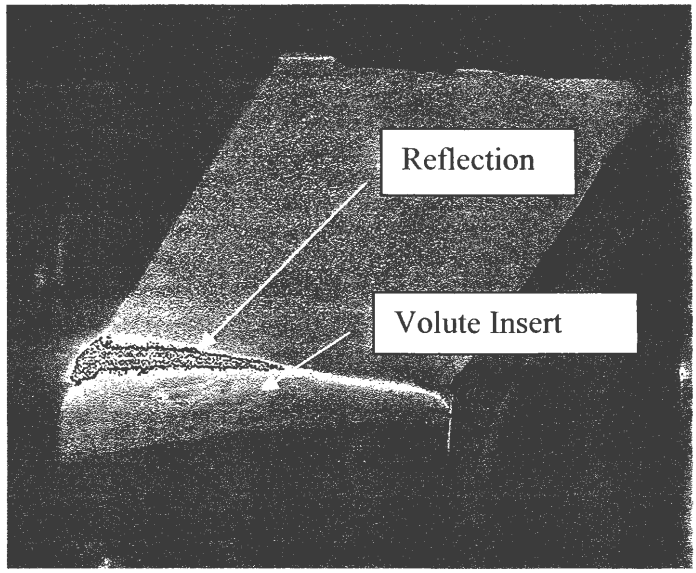

Figure 3.2 PIV Image with Light Sheet Impinging on Volute Insert

The experiments with the volute inserts proved especially challenging since the insulating foam material that the volute insert was made from increased reflection problems. The foam cells were very efficient at scattering any light that they received. Various paints and coverings such as electrical tape and modeling clay were attached to the volute surface in an attempt to reduce reflections, with some success. In future experiments, other methodologies should be pursued to further reduce the effects of reflections from the volute surface. For example, LaVision refers to light absorbing paint in their literature but none was obtained for use during the work reported in this thesis due to time constraints; instead flat black paint was used. Another possibility for improving image quality is to provide an exit window for the light sheet to exit the test section instead of having it simply be absorbed and reflected from the top wall of the test section. However, this was not attempted during these experiments since the presence of the radiators directly above the blower housing assembly meant that any light passing though the exit window would most likely be reflected or

scattered back through the exit window and into the test section by the radiator. Future experimental geometries or conditions may make such a modification possible.

3.4 Triggering

Because the flowfield through the blower housing assembly is expected to vary as the fan rotates, it was important to design the PIV experiments so that data could be collected for fixed fan blade positions. This was accomplished by configuring the system with a shaft encoder to provide a trigger signal to the PIV data acquisition system. The PIV system could then be set to take data at an internally generated rate or by a signal from the shaft encoder.

Data collected using the internally generated trigger gave a random sampling of flow vectors (i.e., uncorrelated with fan blade position) since the test stand shaft and PIV system cycled at different rates. This type of data collection could provide a "time average" of flow through the blower housing assembly irrespective of given fan positions.

Data could also be taken at a specified fan shaft position by calculating and setting a delay time needed after the shaft encoder signal and then using the shaft encoder signal to externally trigger the PIV acquisition system. This type of data collection was used to generate "motion pictures" of the time varying flow through the blower housing assembly and was useful for identifying time varying and periodic phenomena. Some examples of the different triggering strategies used in this study and the corresponding velocity vector fields are presented in the next chapter.

4 RESULTS AND DISCUSSION

4.1 Three PIV Measurements over One Blade Passage

The first trial run of the triggering system consisted of determining three successive ensemble averaged velocity fields during the passing of a single fan blade. The objectives of this set of experiments were to: 1) validate the operation of the triggering system, and 2) to determine if any vortical structures or velocity pulses appeared in the mean velocity fields, indicating a repeating, periodic phenomenon associated with the passage of the fan blade. Three vertical planes, each within the left and right hand side of the blower housing, were selected for PIV analysis, Fig. 4.1.

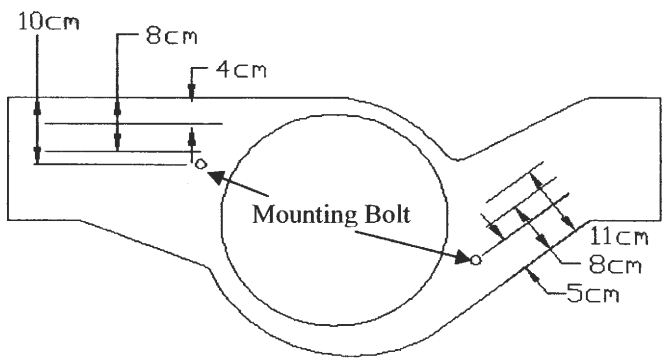

Figure 4.1 Vertical Planes for Baseline PIV

The planes were chosen in an attempt to measure flow at three different locations across the width of the blower housing. The spacing between the planes was not constant since flow behind the mounting bolts was also of interest, and thus two of the planes were placed directly downstream of the bolt. Ensembles of 1500 PIV images were taken on each of these planes for three different fan positions over the passage of one fan blade. Triggering delays of 0, 694.4 microseconds, and 1388 microseconds were set to obtain the data sets for the three fan positions. The fan rotation rate was 3200 rpm.

The windows in the blower housing were not illuminated completely in this initial setup since the light sheet was not wide enough for full coverage. Data from the entire window were obtained by measuring each set of conditions with the light sheet adjusted to cover one side of the window and then the other, creating a mosaic view of the flow over the entire region of the window. Later, it was found that cylindrical lenses could be used in series to obtain a wider light sheet, allowing all the data to be collected at one time. The methodology using the wider light sheet was used to collect results presented later in this thesis.

Fig. 4.2 provides example data from three raw PIV images along with the vector field produced from each. Figure 4.2(a) is a schematic of the cross section of the blower housing assembly indicating the location of the measured velocity fields within the blower housing. Figures 4.2 (b), (d), and (f) are examples of raw PIV images collected at the three fan positions, demonstrating the location of the light sheet within the blower housing and incidence of reflection and scattering of laser light from the solid surfaces and windows. The scattered light in the raw images illuminates the rotating fan blade on the left side of each of the images and allow the changing position of the fan blade to be observed over the

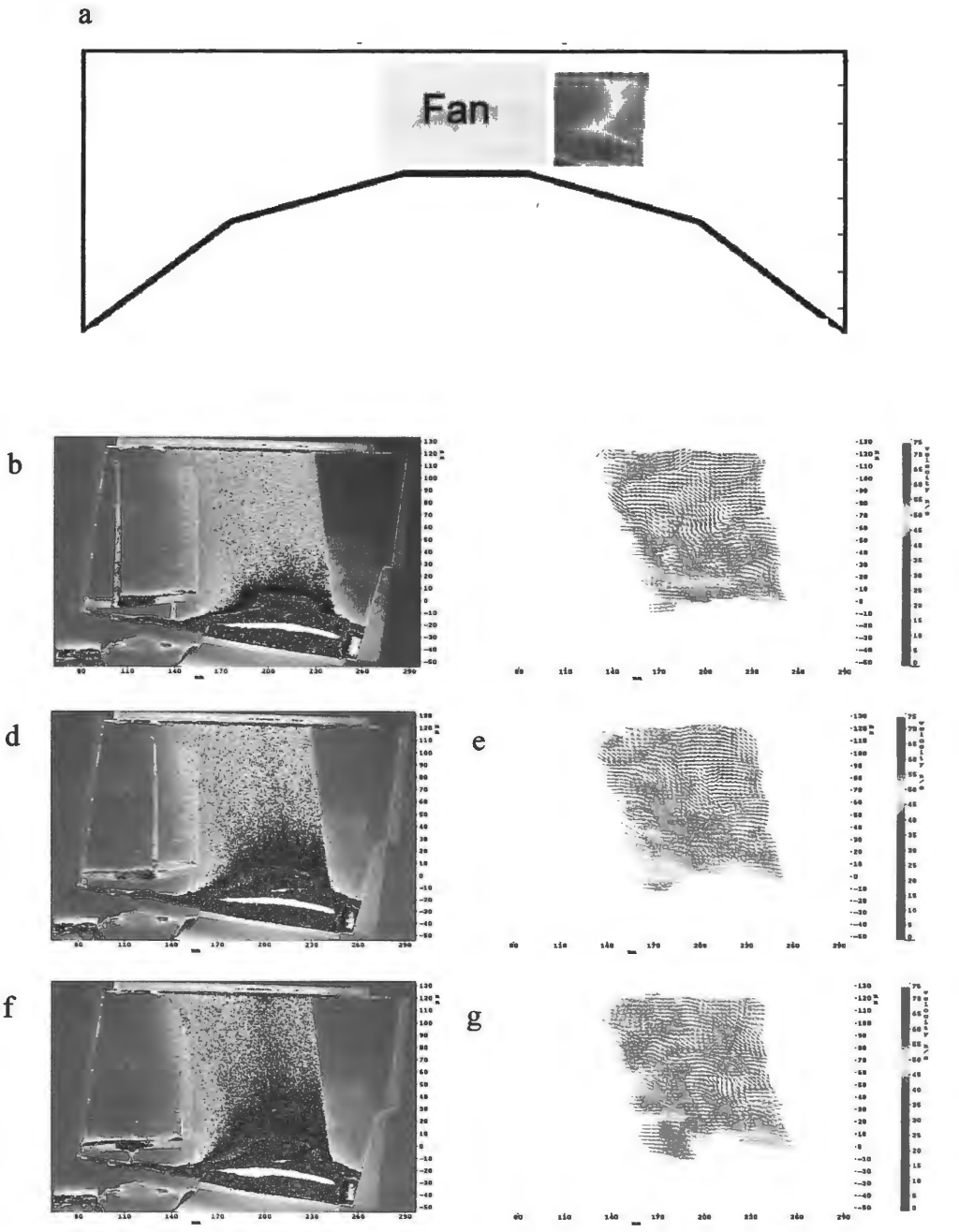

Figure 4.2: PIV Images and Vectors Over Three Fan Positions on the Right Hand Side of the Blower Housing (a) Cross Section of Blower Housing Showing Orientation, With Vectors (b) Image at 0 second Delay (c) Vectors at 0 second Delay (d) Image at 694.4 microseconds Delay (e) Vectors at 694.4 microseconds Delay (f) Image at 1388 microseconds Delay (g) Vectors at 1388 microseconds Delay

three triggering conditions selected. Figures 4.2 (c), (e), and (g) are the instantaneous velocity vector fields measured from the raw images shown in Figs. 4.2 (b), (d), and (f), respectively. In actuality, a pair of raw images is necessary to obtain a single velocity field, but only a single image is shown here. The succession of these velocity vector fields shows a surge of higher speed air developing on the left side of the vector field in Fig. 4.2 (c), halfway across the field in Fig. 4.2 (e) and completely covering the field in Fig. 4.2 (g). The lower part of the vector field, corresponding to the base of the fan, shows the highest absolute velocities. These velocity surges associated with blade passage are a potential source of tone noise since they occur at regular intervals. Air speeds between 15 and 65 meters/sec are typical in the areas investigated. Also note that higher speeds are seen near the fan and low in the blower housing.

The greater flow off the base of the fan, low in the blower housing, resembles the flow system described as von Karman's viscous pump in which fluid adjacent to a rotating disc is pulled along with the disc circumferentially. The fluid moves radially outward in the absence of a force sufficient to keep it to the circumferential path. This fluid is replaced by fluid moving axially toward the rotating disc (White 1991).

This flow pattern is also similar to the flow predicted by CFD for the fan used by Meakhail and Park (2005) when it is operated with the flow restricted, in that both fans show higher velocity near the fan base. Speeds are generally more uniform farther from the fan as might be expected.

Figure 4.3 shows PIV vectors with part of the x-component of velocity subtracted to disclose vortices in the flow. This subtracted velocity is termed the *convective* velocity since it represents the velocity at which the observed large scale structures are moving through the

flowfield. Individual PIV vector plots typically show vortices at varying locations. These vortices are a potential source of broadband noise, since they do not occur at a single fixed frequency, but instead occur over a broad range of frequencies.

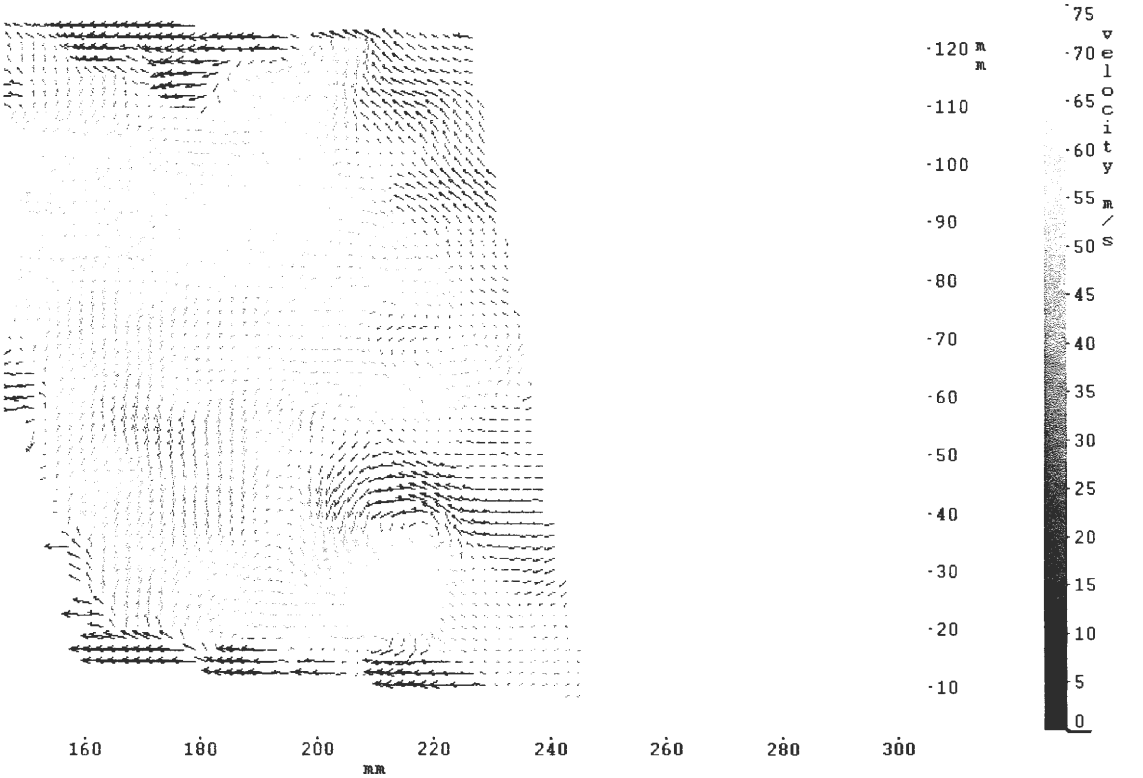

Figure 4.3 Vectors from a Single PIV Image

Vortices also are visible in the ensemble-averaged PIV vector fields. Figures 4.4 through 4.7, which also have a convective velocity subtracted from them, show a vortex as it moves through the blower housing. These are ensemble averages of 1500 realizations of the velocity vector field. The first three velocity fields are shown in sequence with delays of 0, 694.4 microseconds, and 1388 microseconds set to cover one fan blade passage in three parts. This vortex continues to convect downstream towards the blower housing exit even after it leaves the field of view of Fig. 4.4-4.6. For example, in Fig. 4.7 an arrow marks this vortex as seen in the ensemble-averaged velocity vector field taken with the right hand side

of the window illuminated. This vortical flow structure is repeatable and periodic as evidenced by its appearance in the average of 1500 images.

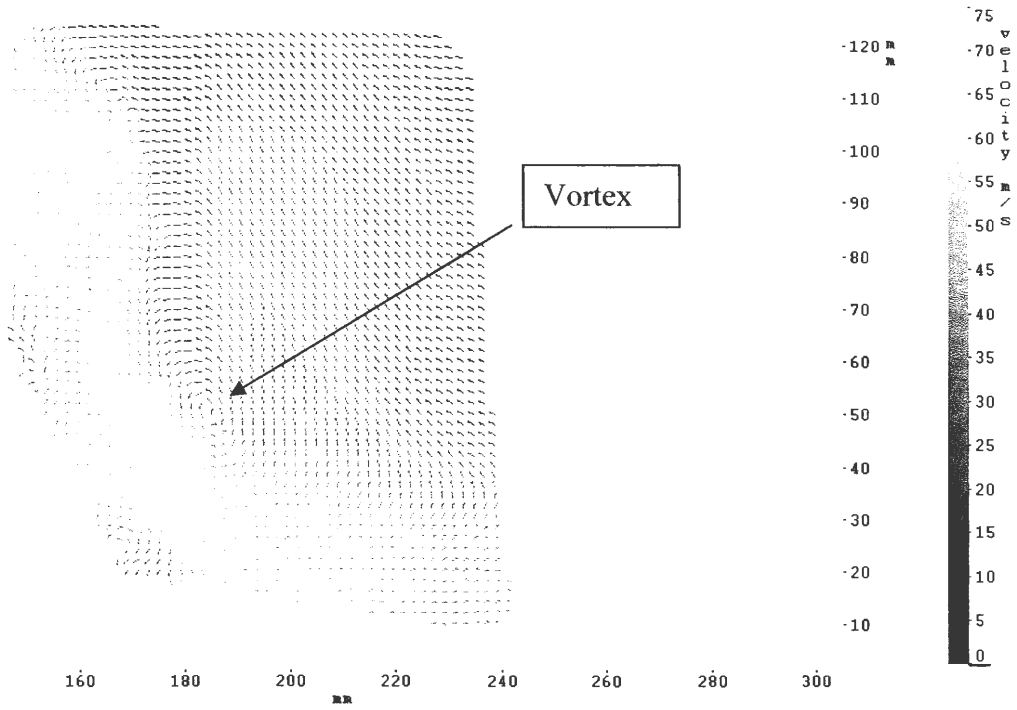

Figure 4.4 Left Side, First Fan Position, Left side of window illuminated

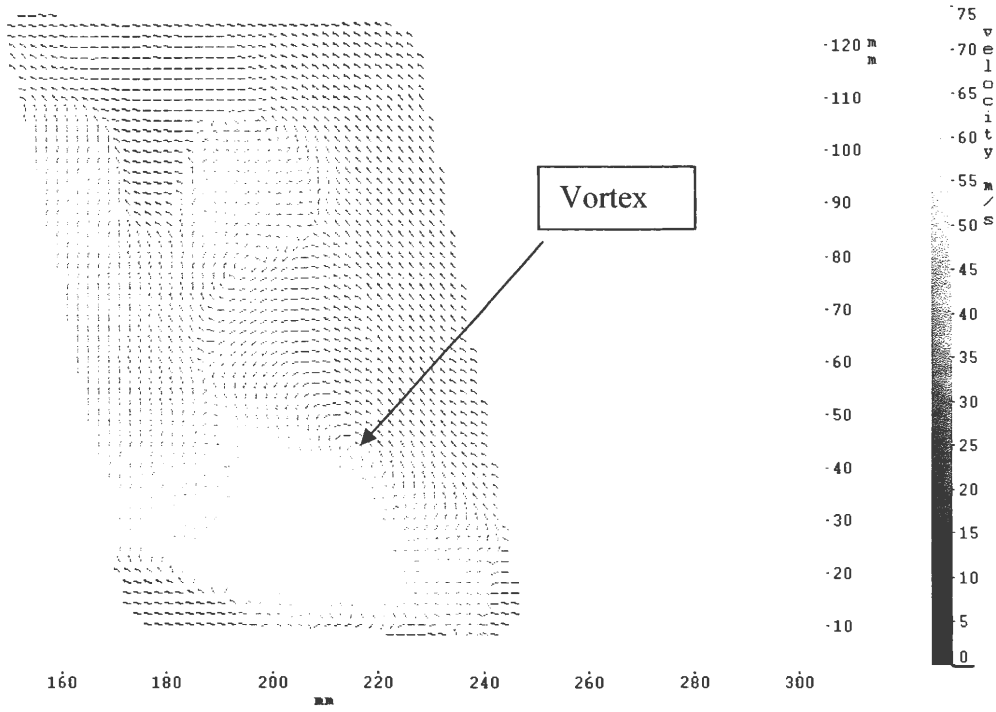

Figure 4.5 Left Side, Second Fan Position, Left side of window illuminated

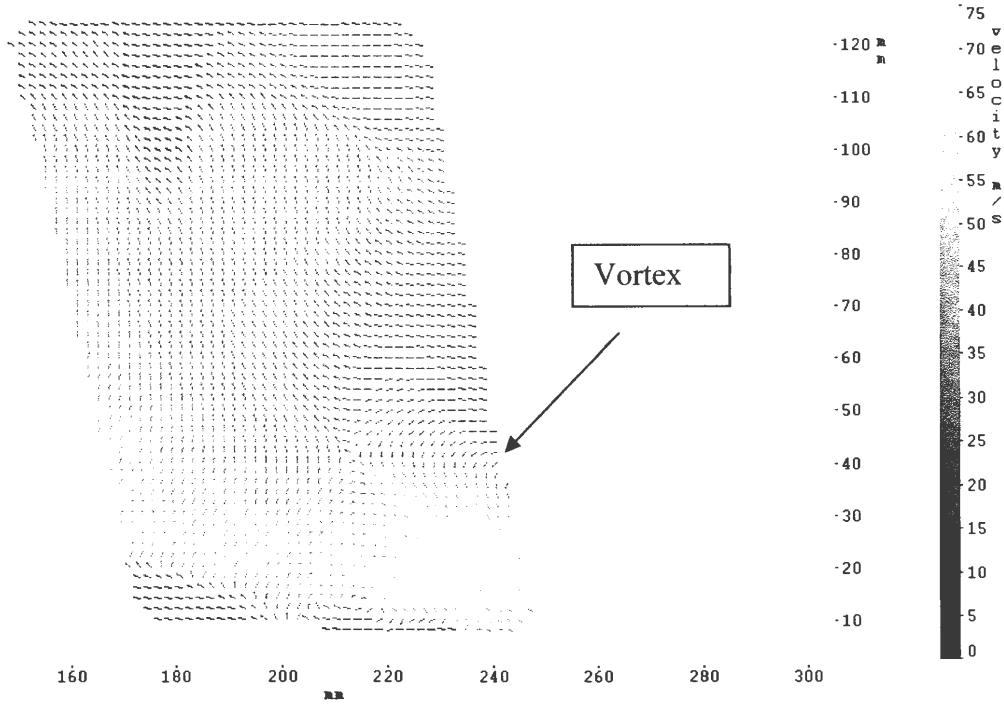

Figure 4.6 Left Side, Third Fan Position, Left side of window illuminated

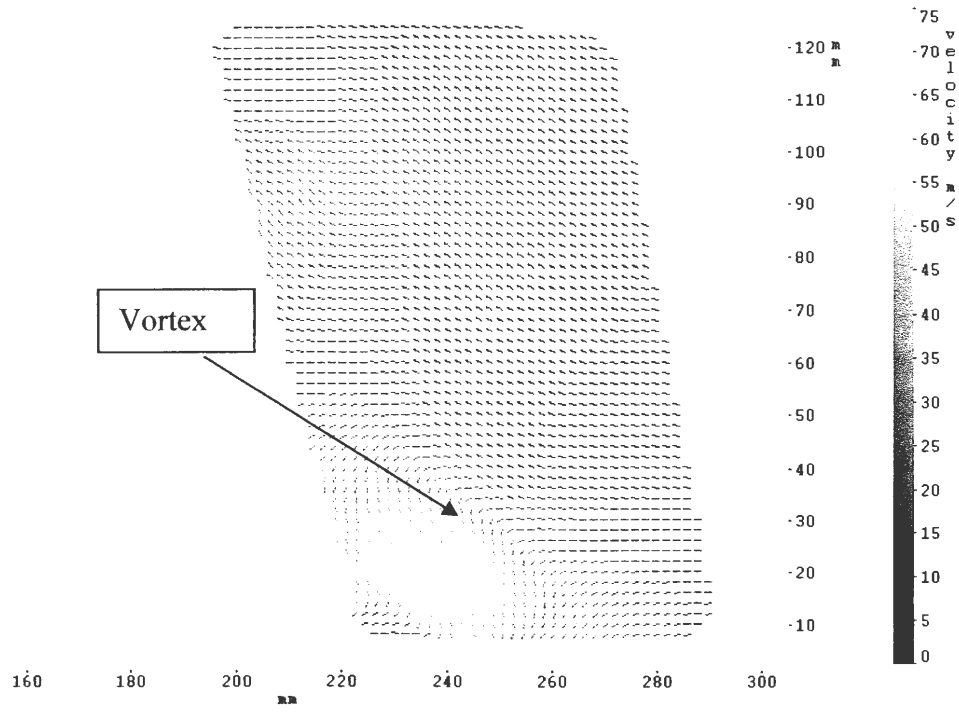

Figure 4.7 Left Side, Third Fan Position, Right side of window illuminated

Figure 4.8 is the same ensemble average of 1500 vector fields shown in Fig. 4.3 but without subtracting the convective velocity. Velocities on the mean plot are between 25 and 55 m/s. Velocities decrease with greater distance from the fan and at higher positions in the blower housing. This figure also demonstrates the importance of subtracting a convective velocity if one wishes to observe structures traveling in the flowfield, as these structures are almost completely indiscernible in Fig. 4.8.

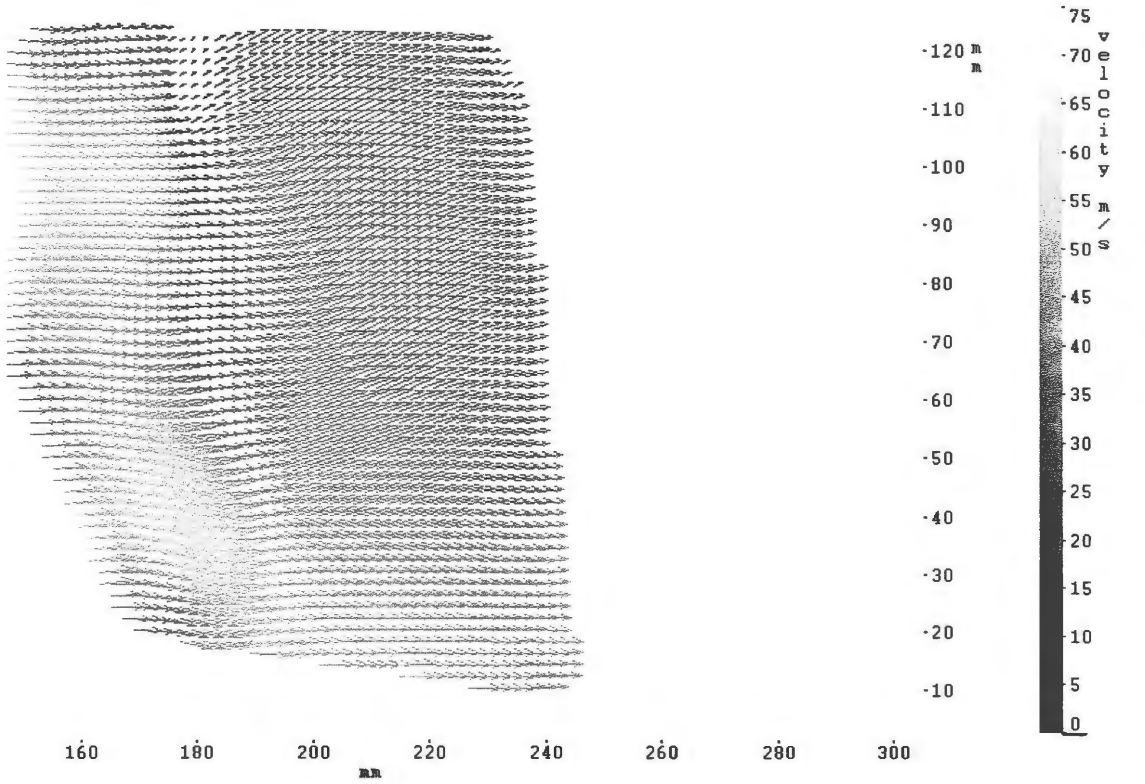

Figure 4.8 Left Side, First Fan Position, Left side of window illuminated

4.2 Five PIV Measurements across 1 Blade Passage

Possible changes to the fan and blower housing and their effects on the flowfield were investigated using PIV to both improve understanding of the system and also to evaluate improvements in air handling performance. In these measurements, a more detailed picture of the flow changes with the passing of each fan blade was desired, so the time required for one blade passage was divided into five parts to obtain a more detailed picture of this flow. The geometry changes investigated included three prototype fan configurations as well as a change to the blower housing assembly shape.

The prototype fans were altered versions of the production fan. In these prototype fans, a change was made to the base geometry of these fans. This specific alteration made to

the fans is proprietary information of the Bobcat Corporation. The prototype fans were also modified by cutting away part of the blades to allow more gradual ingestion of the air entering the fan. Two of these prototype fans were equipped with rings that were attached to the tops of the blades. Two sizes of ring were used. The larger ring was designed so that the exit and entrance areas of the fan were the same in an attempt to obtain a more uniform flow throughout the system. The smaller ring was included to test the effect of varying ring geometry.

The prototype fans were tested both with and without an insert which modified the shape of the blower housing. The insert was fitted within the left hand side of the blower housing and provided a volute shape similar to that on the right hand side of the housing. The hypothesis behind the altered blower housing shape was that it would confine air to the fan blades for a longer time and hence increase pressure at the right hand outlet.

PIV experiments were performed on single vertical and horizontal planes within the blower housing. The location of these measurement planes are shown in Fig. 4.9. Ensembles of 1000 PIV images were taken at each of five fan positions. The fan positions were separated by intervals of 400 microseconds starting from the minimum system delay. This provided coverage of the passage of one fan blade in five steps.

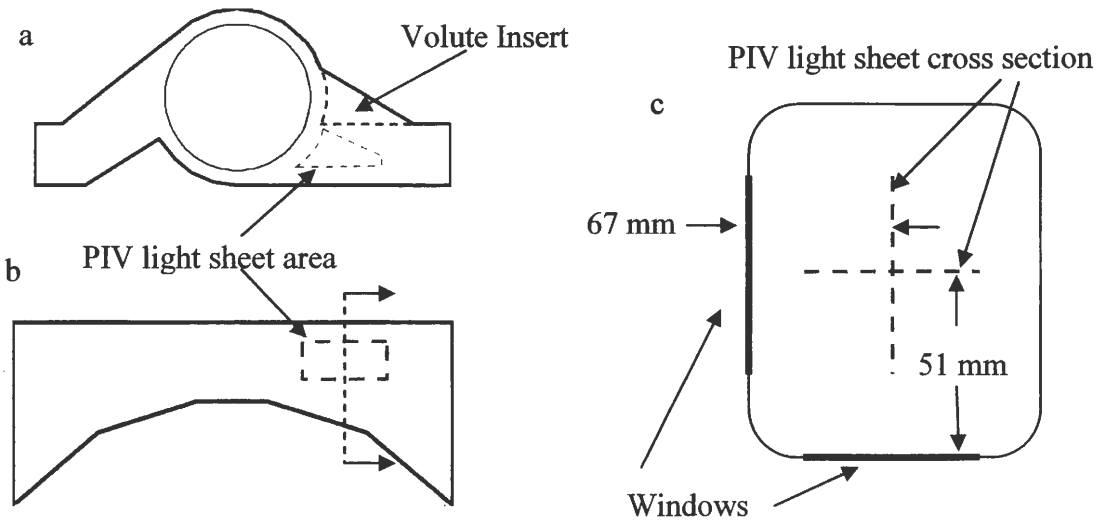

Figure 4.9 PIV Plane Locations, (a) Top View, (b) Frontal View, (c) Cross Section (End View)

This testing was completed on the left hand side of the blower housing only. Time constraints and difficulties with reflections prevented the completion of observations on the right hand side of the blower housing as was originally planned.

The data from these observations were analyzed by viewing the series of five mean PIV vector fields for five sequential fan blade positions to aid in understanding how flow varied with the passing of each fan blade. Velocity profiles across the PIV vector field at differing distances downstream from the fan were prepared to assist in comparing flow under different conditions. The standard deviation of flow velocity along the profiles was used to estimate flow uniformity.

Figure 4.10 consists of a sequence of five corresponding vertical and horizontal PIV velocity fields. The test conditions for Fig. 4.10 were for a prototype fan with the altered base geometry but with no ring and with the volute insert installed.

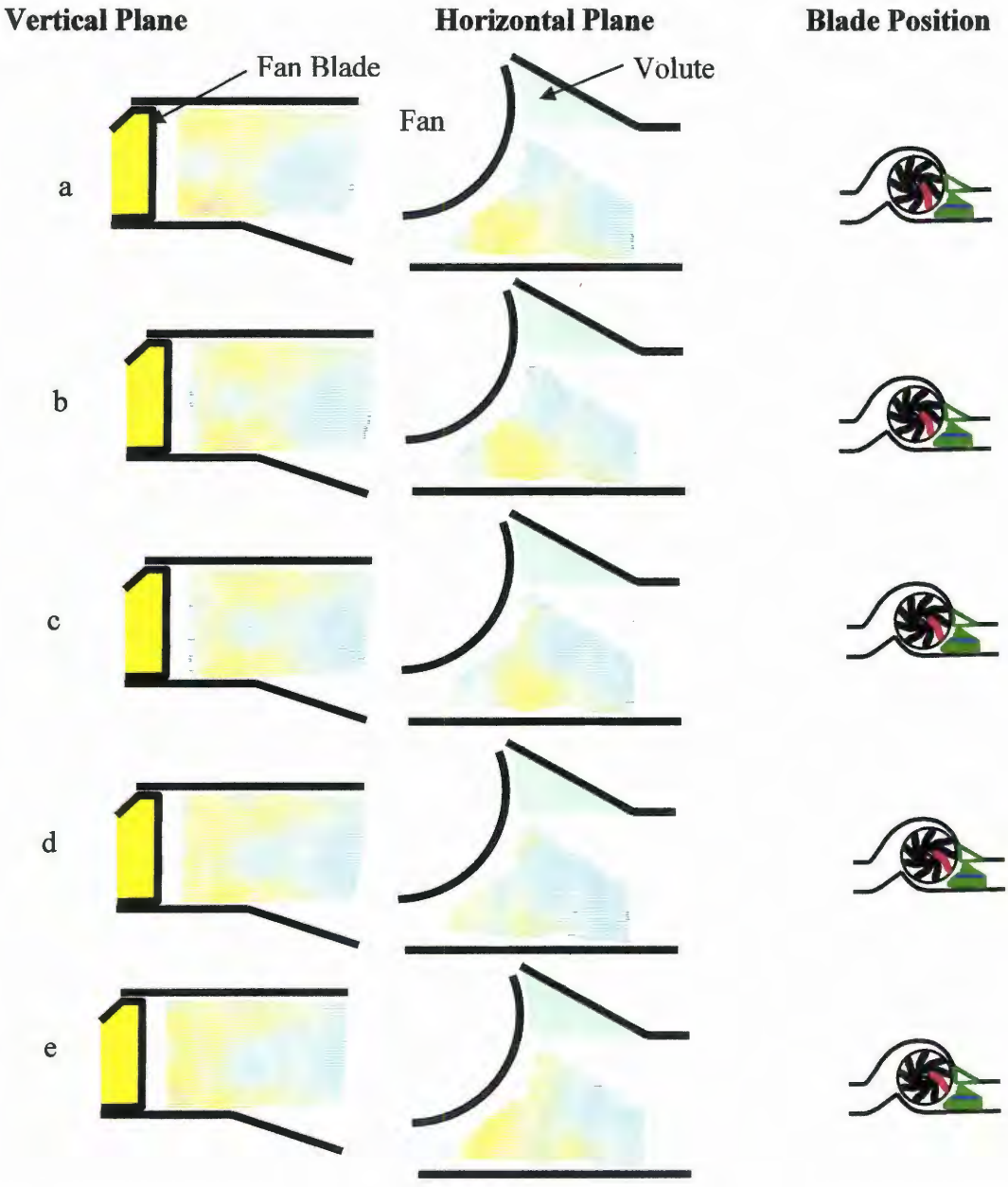

Figure 4.10 Ensemble averages of 1000 velocity fields, Vertical and Horizontal Planes, Prototype fan with no ring, Volute installed, Five fan positions over one blade passage: a through e

The PIV mean vector fields presented are ensemble averages of 1000 individual vector fields. A representation of the fan blade position is provided with the corresponding PIV images.

Sequences of ensemble-averaged velocity vector fields, such as those in Fig. 4.10, are useful for identifying periodic behavior in the flowfield over the passing of a fan blade. For example, a pulse of higher velocity air is visible in the lower left corner of Fig. 4.10 (a) – (c) in the vertical plane images. This pulse can be observed to traverse from left to right in these three vertical vector fields. The vertical vector fields in Figs. 4.10 (d) and (e) show a new pulse beginning at the lower left. Also in these later images, the initial pulse seen in Figs. 4.10 (a)-(c) is weakening as it continues further to the right. A similar pulse can also be seen in the corresponding horizontal views, again at the lower right with the same behavior in sequential vector fields. This pulsation as air is shed from the fan blades is potentially very important as it may be a source of noise.

Two regions of higher flow velocities are seen near the upper and lower borders of the vertical images, separated by a central region of lower velocity. The horizontal view has a region of higher velocity on the side of the image furthest from the volute. Non-uniformities in the velocity field are a source of shear stress in the flowfield. The shearing between the regions of lower and higher velocity generates turbulence and is a potential source of noise. *Comparison to the variation in velocity as seen in PIV results, such as those in Fig. 4.10, suggests that the fan is operating at a lesser flow than could be produced without restriction at the inlet.* Further work by Meakhail and Park (2005) showed that a less restricted inlet flow resulted in uniform velocity along the full depth of the fan blades in a centrifugal blower.

Figure 4.11 shows a comparison of ensemble-averaged velocity fields in the vertical plane both with and without the volute and using the prototype fan with no ring. Note that the areas covered by the PIV vector fields for these two views differ slightly because the data without volute were taken with the laser light sheet introduced through the lower horizontal window while for the view with the volute the light sheet was introduced through the discharge port. A small triangular region in the lower left side of the vector field was not lighted in the image with volute because the light sheet, introduced through the lower window, was angled slightly.

The vector fields shown in Fig. 4.11 contain pulses of higher velocity air similar to those seen in Fig. 4.10. Higher velocity flow is seen at the top and bottom of both views with a lower velocity central region. Again shear between these regions is a possible source of noise.

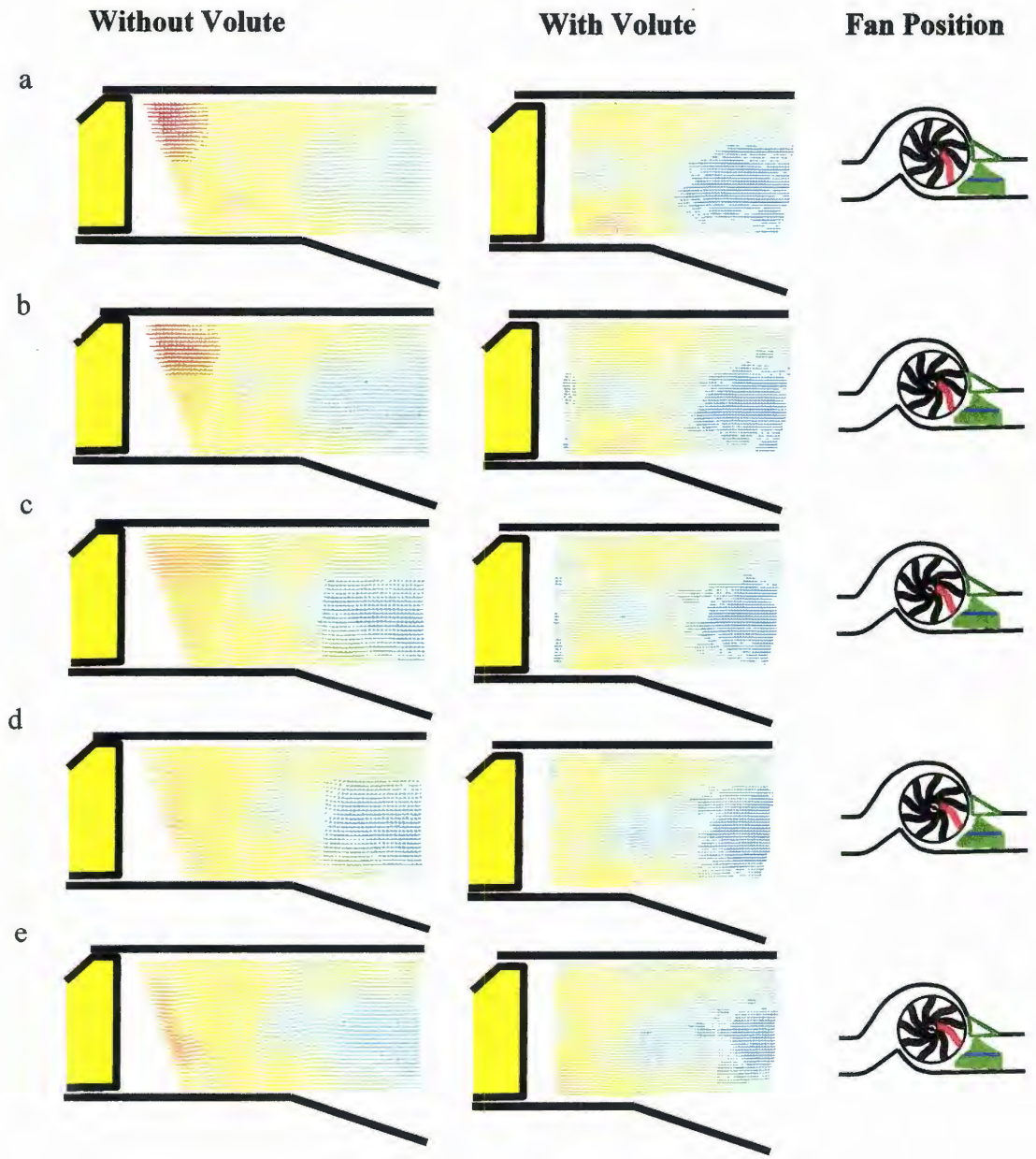

Figure 4.11 Ensemble averages of 1000 velocity fields, Vertical Plane, Prototype fan with no ring, with and without Volute installed, Five fan positions over one blade passage: a through e

Figure 4.12 shows velocity field data for flow in blower housing assemblies with the volute insert installed for fans both with (right) and without (left) the large fan ring modification. The addition of the fan ring results in substantial changes to the observed flowfield. First, the flowfield for the fan without the ring shows a strong higher velocity region near the base of the fan, and a "weaker" high velocity region near the top of the fan. The addition of the fan ring results in the strengthening of both of these high velocity regions, particularly the high velocity region near the top of the fan. These high velocity regions are not steady, but instead appear to be dependent on fan blade position, with the air coming off the fan blades in pulses. For example, a pulse of higher velocity air begins to leave the fan blade in Fig. 4.12 (b) for the fan with the ring installed and convects downstream through views (c), (d), and (e). Between the time of view (e) and (a), the pulse has convected past the point where the area of the blower housing assembly increases, and this increase in area results in a deceleration of the flow and a subsequent weakening of the pulse. Frame (a) is also for a time just before the next high velocity pulse is shed from the fan blade. This pulsing behavior is also observed for the fan without the ring attachment, but the pulse is weaker and the phase of the pulsating flow is shifted. The pulsing behavior associated with blade passage is approximately 400 microseconds later with the ring installed. The pulsing behavior is significant, because it is a possible source of noise within the blower housing assembly.

The variation in velocity again suggests that the fan is operating at a lesser flow than could be produced without restriction at the inlet, as was observed in the Meakhail and Park (2005) CFD results. With the large fan ring in use, flow is more uniform across the depth of the fan.

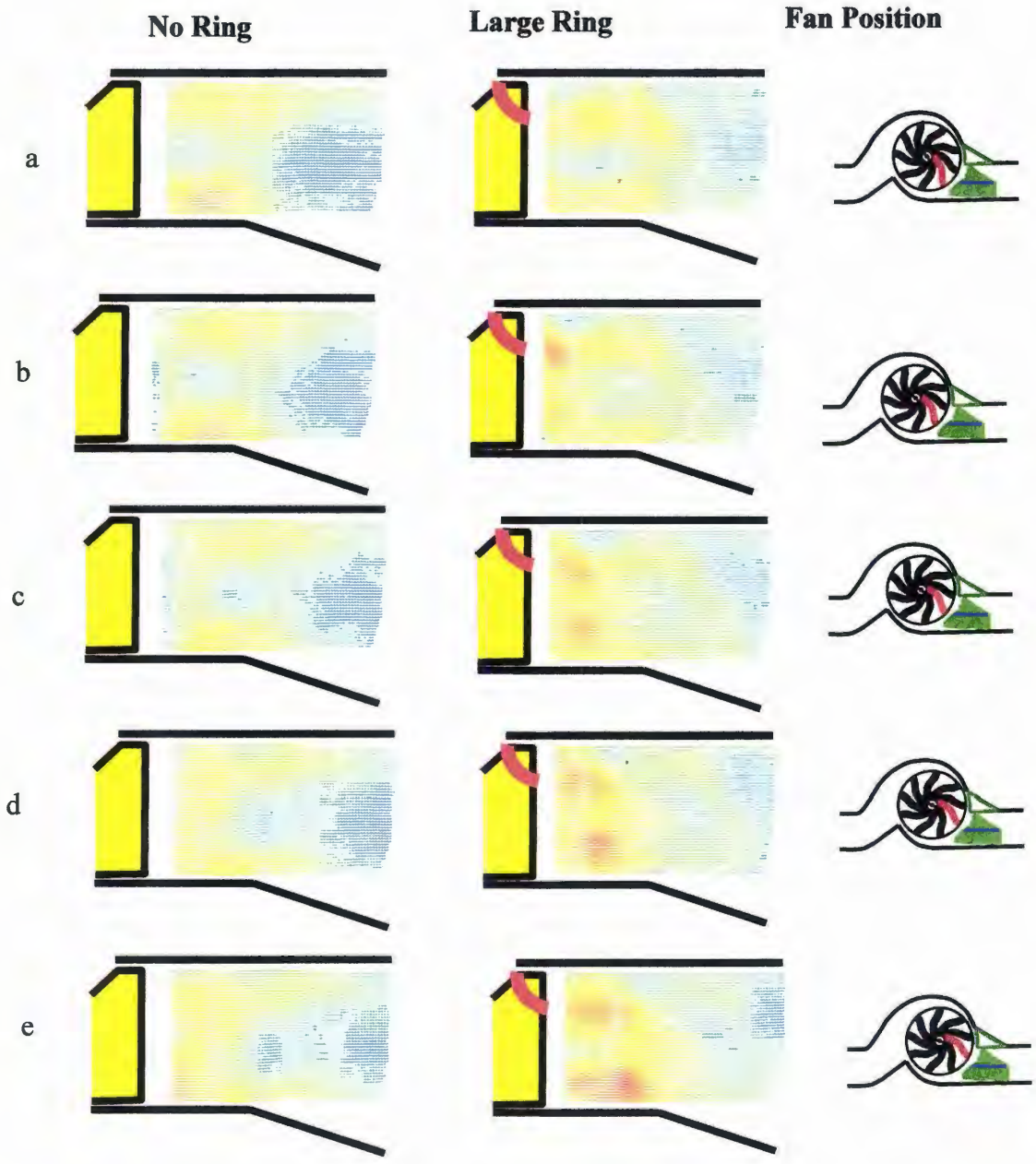

Figure 4.12 Ensemble averages of 1000 velocity fields, Vertical Plane, Prototype fan without ring, Prototype fan with large ring, Volute installed, Five fan positions over one blade passage: a through e

The higher velocity regions in both flows seem to dissipate into a more uniform pattern about halfway across both views. This is due to the area increase of the blower housing assembly at this location. The area increase decelerates the flow. The non-uniformity observed in the flowfield for both fan geometries is significant because the non-uniformities result in high-shear regions that can generate turbulence, and potentially cause noise. Although areas of possible noise generation by flow shear due to velocity variations appear more likely with the ring installed, sound power testing, ANSI S12.36-1990 (R 1997), indicated that the large fan ring reduced noise by approximately 1 dbA, Fig. 4.13. This highlights the difficulty of drawing strong conclusions about the flow from a single plane of PIV data in a highly three-dimensional flowfield such as in the present experiments.

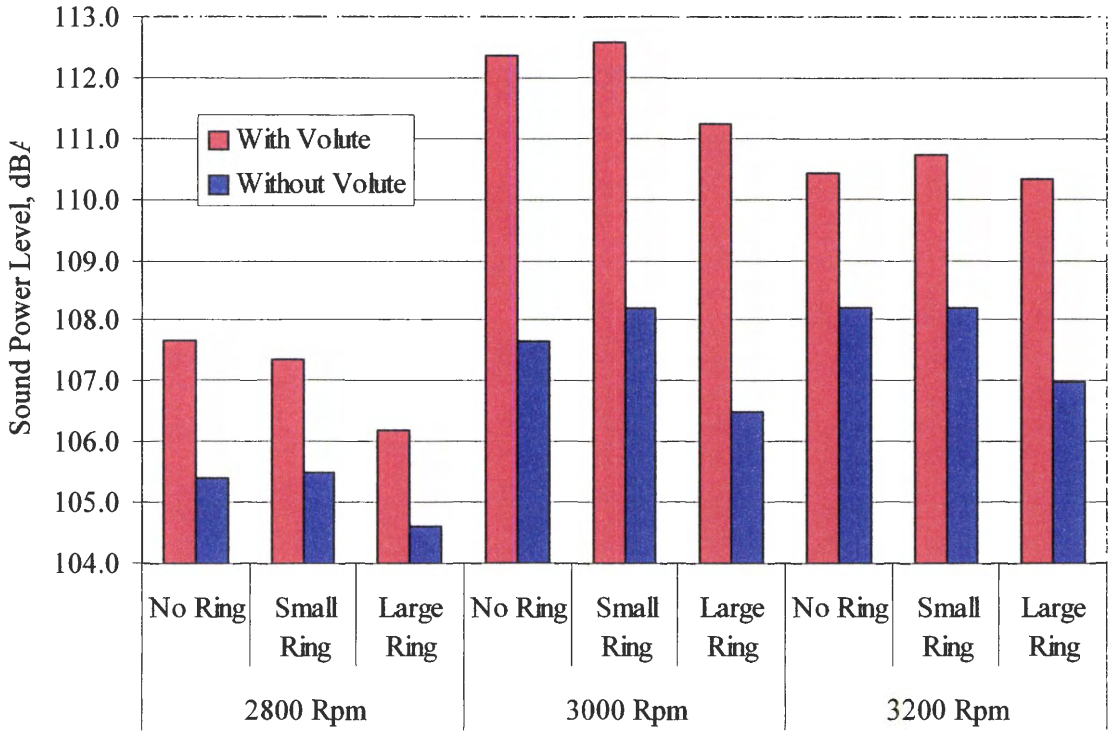

Figure 4.13 Sound power measured with a four microphone substitution method. ANSI S12.36-1990 (R 1997)

The sound power data in Fig. 4.13 shows a significant increase with the volute insert installed. This increase can be explained by the introduction of the volutes tongue in proximity to the fan where previously none was present as shown by (Velarde-Suarez, S *et al*. 2000) and Chu, Dong, and Katz (1995b). Also, the fan with the small ring produces more noise than the fan with the large ring, which is consistent with the conclusion by Fehse and Neise (1998) that a fan shroud (ring) with a smaller radius of curvature can result in increased noise production caused by flow separation.

4.3 Twenty Seven PIV Measurements Over One Fan Revolution

The design of the fan common to these experiments included nine unevenly spaced blades. Observations of flow from all the blades were needed to determine whether there was significant flow variation between the blades. In an attempt to measure flow changes over the entire revolution of the fan, the time needed for one revolution of the fan was divided into 27 parts, three divisions for each blade, using evenly spaced triggering delays of 694.4 microseconds. This scheme provided information on flow from all the blades, but due to the uneven blade spacing not all blades were observed at the same angle. These observations were made on the right side of the blower housing on a vertical plane centered in the blower housing. Figures 4.14 and 4.15 contain the vector fields measured on the right-hand side of the blower housing in the sequence of 27 using the production fan and the fan with large ring and volute insert installed. The sequences of vector fields shown in Fig. 4.14 and 4.15 both show pulses of higher velocity air crossing the vector field as the sequence of images is followed through one cycle of the fan.


1


2


3


4


5


6


7


8


9


10


11


12


13


14


15


16


17


18


19


20


21


22


23


24


25


26


27

Figure 4.14 Twenty seven sequentially numbered vector fields, evenly spaced triggering through one fan revolution, Production fan and Blower Housing

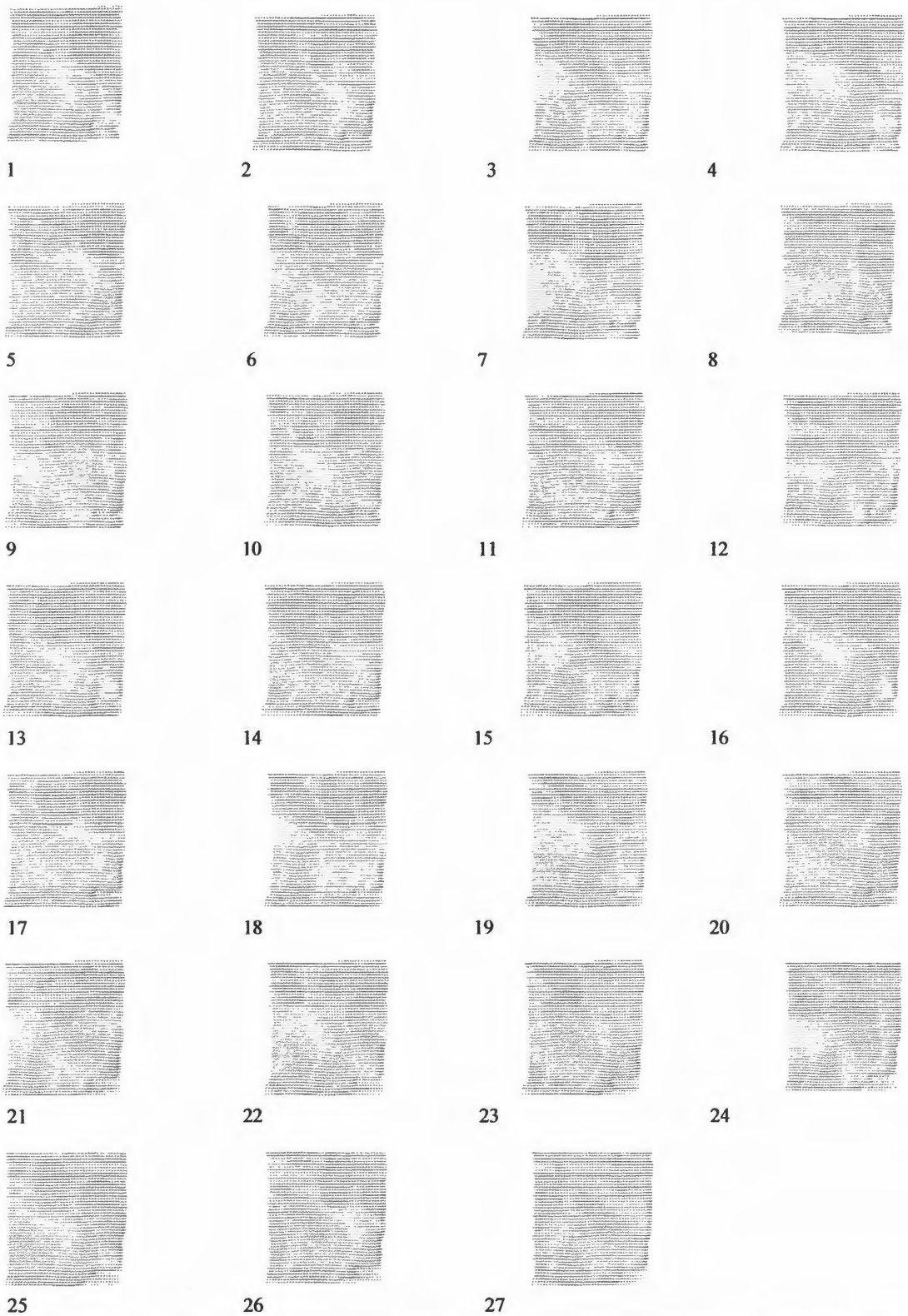

Figure 4.15 Twenty seven sequentially numbered vector fields, evenly spaced through one fan revolution, right side, fan with ring and volute

Flow velocity is higher near the bottom of the blower housing with both the production fan and blower housing and the fan with large ring and blower housing with volute insert installed. The pulses of higher velocity air reach higher into the blower housing with the production fan and blower housing. The fan with large ring and blower housing with volute insert combination shows higher velocity pulses restricted to approximately the lower half of the velocity field, but these pulses are wider regions of high speed air separated by a narrower region of lower speed air, compared to the pulses generated with the production fan and blower housing. This more continuous character of flow could account for reduced noise production when using the fan with large ring since shear (and thus turbulence) in the air flow would be reduced.

Flow differences between individual fan blades were studied by determining the position of each fan blade at each trigger position. Data from each trigger position were classified based on the angular offset from an arbitrarily chosen fan blade which was near the PIV observation area at the first trigger position. Data from each triggering were then grouped so that blades within 5 degrees of the same angular position relative to the chosen fan blade could be compared. Since the fan blades were spaced unevenly, data could be grouped over 40 degrees in 3 to 5 degree increments in this manner. Velocity profiles at a 160 mm offset from the fan shaft are shown in Fig. 4.17. Although all blades were not tested in all positions, the available data suggests that the blades are performing similarly.

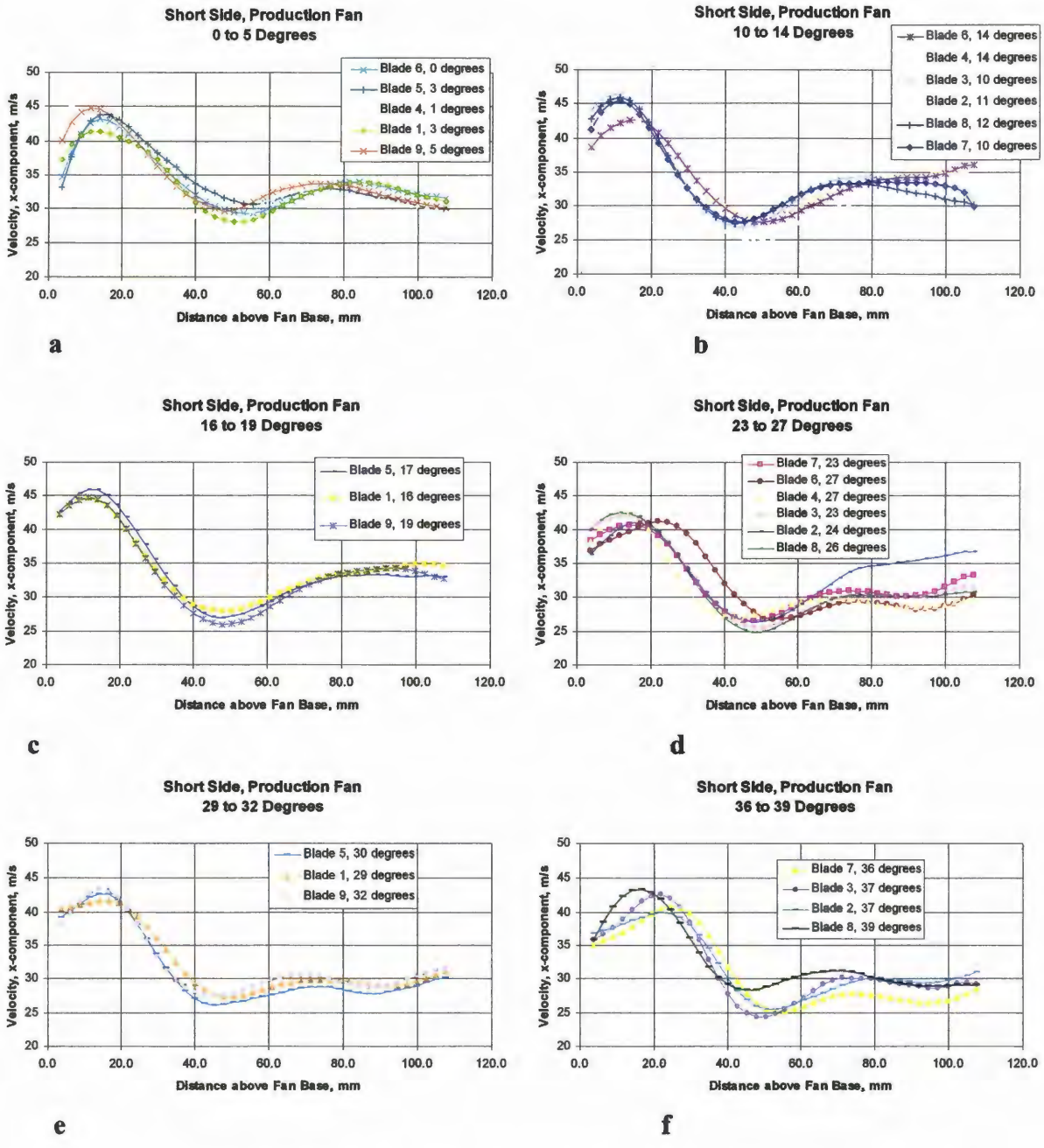

Figure 4.16 Velocity Profile at 160 mm from fan, grouped according to angle from the nearest blade, Production Fan: (a) 0 to 5 degrees, (b) 10 to 14 degrees, (c) 16 to 19 degrees, (d) 23 to 27 degrees, (e) 29 to 32 degrees, (f) 36 to 39 degrees

As can be observed in Fig. 4.16, the flow profiles are similar within each group indicating nearly uniform blade performance. Notice that the higher velocity flow is low in the blower housing with slower flow at upper levels. This is consistent with the vector fields presented in Fig. 4.14. Further investigation could explain the minor variations seen in Fig. 4.16 (d) and (f). Since the blade spacing is variable, the preceding or following blade could be causing the differences in the outlying traces. Experimental error is also a possibility.

Figure 4.17 contains groups of comparable velocity profiles for the fan with large ring with volute insert installed in the blower housing. Here the velocity is also high near the bottom of the blower housing, however it is also higher near the middle of the vector field. Figures 4.17 (a), (b), (c) and (d) show two velocity peaks with the highest velocity near the center of the field. Figures 4.17 (e) and (f) show a shift of the higher velocity peak towards the center of the vector field, although the peak is not as pronounced. These plots also are quite similar when grouped with respect to blade position which again indicates that the flowfields generated by the passing of each of the nine fan blades are very similar.

The two changes to the production air handling system which comprise the system with large fan ring and volute (that is the fan geometry changes and the altered blower housing shape) influence flow in different ways. The fan ring focuses the high velocity region near the center of the vertical velocity profile. The volute insert retains air in the fan longer. The contributions of each change to the resulting air flow are somewhat entangled. This matter could be addressed in a future study.

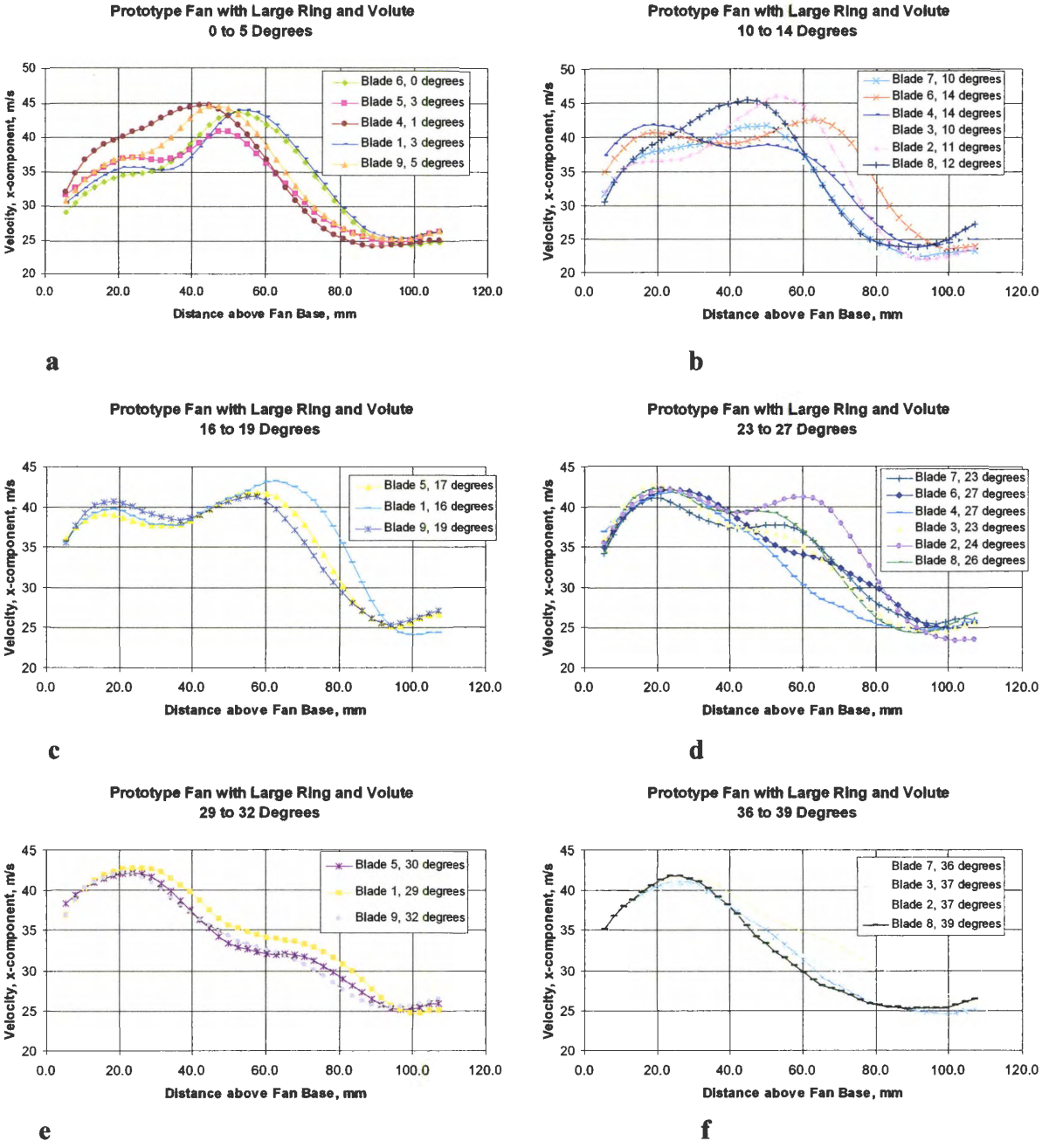

Figure 4.17 Velocity Profiles at 160 mm from fan, grouped according to angle from the nearest blade, Prototype Fan with Large Ring and Volute: (a) 0 to 5 degrees, (b) 10 to 14 degrees, (c) 16 to 19 degrees, (d) 23 to 27 degrees, (e) 29 to 32 degrees, (f) 36 to 39 degrees

Figure 4.18, (a) and (b) shows all twenty-seven x-component velocity profiles on one plot for the same fan/blower housing combinations presented in Figs. 4.16 and 4.17. The traces on the plot from the production fan velocity fields occupy a band about 10 m/sec wide while those for the fan with ring and volute insert installed occupy a 15 m/sec band, indicating less flow uniformity with the fan ring and volute. This less uniform flow could result in increased noise production; however, since sound testing, Fig. 4.13, shows less noise for the fan with ring, again the difficulty of drawing conclusions based on a single plane of PIV data is emphasized.

Further evaluation of the cooling package flow through one fan cycle was performed by constructing surface plots of x-component velocity profiles at 120 mm and 160 mm offsets from the fan shaft. These plots show the x-component velocity profiles from the vector plots obtained at 27 equally spaced fan positions in sequence as a contour plot. In these plots all the x-component velocity information through one fan cycle can be observed in a single figure, making it easy to investigate changes in the flow over time.

Figure 4.19 contains plots at 120 mm (a) and 160 mm (b) offset for the production fan and blower housing. Blade passages appear as ridges on the surface plot. The higher velocity flow near the bottom of the blower, which was pointed out earlier, is also evident in these plots. The low velocity region approximately 45 mm above the fan base is seen on both of these plots. The drop in velocity in the central part of the vector field is more pronounced in the plot at 160 mm. Figure 4.20 contains plots identical to those discussed in the preceding paragraph excepting that the plots in Fig. 4.20 were made from data for the fan with large ring and volute. The flow is somewhat smoother in Fig. 4.20 (b) at 160 mm offset from the fan shaft than at 120 mm, Fig. 4.20 (a).

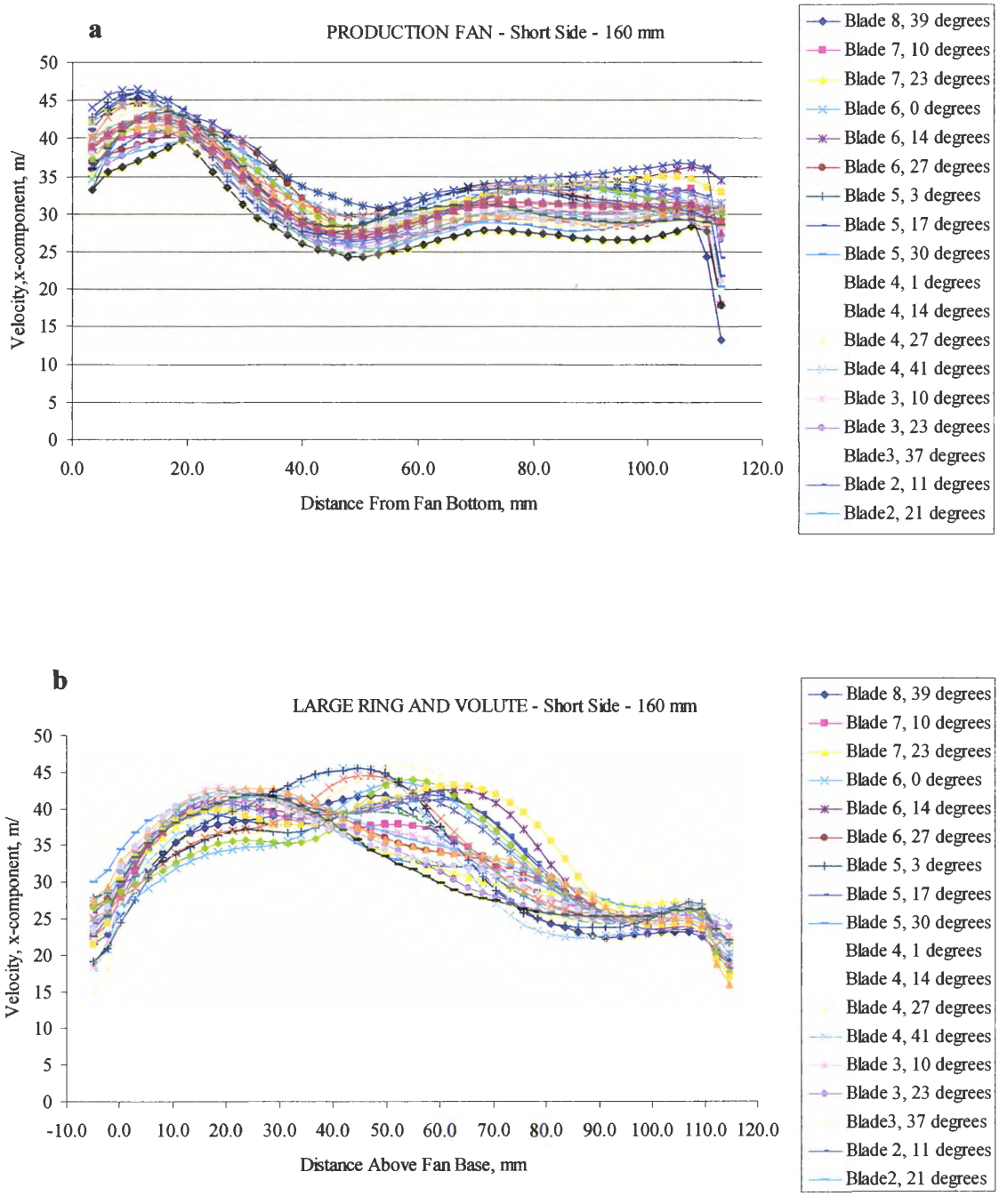

Figure 4.18 Velocity Profiles for One Turn of the Fan, (a.) Production Fan, (b.) Fan with Large Ring and Volute

a.

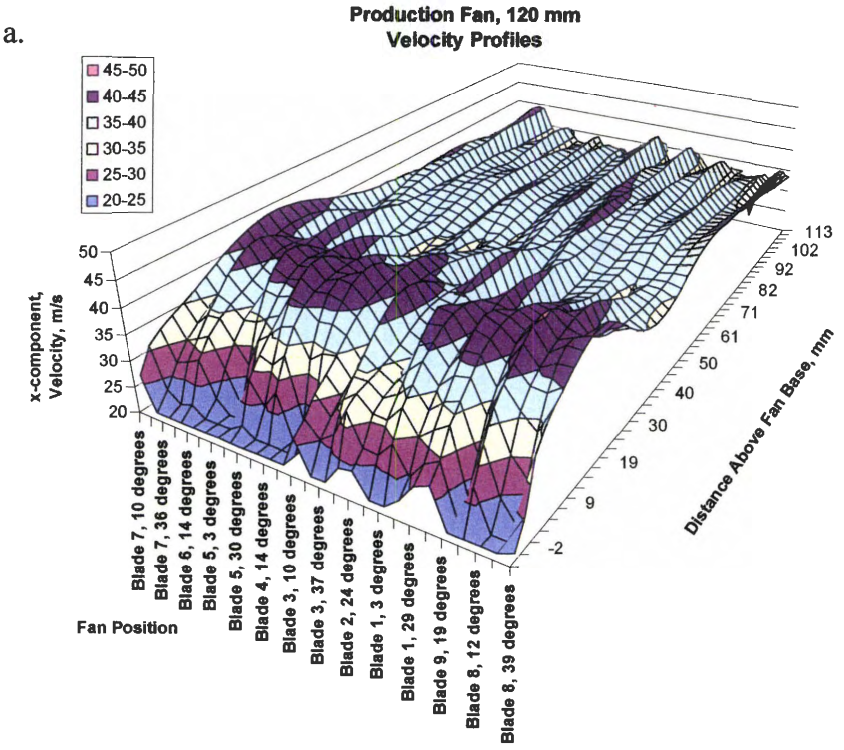

b.

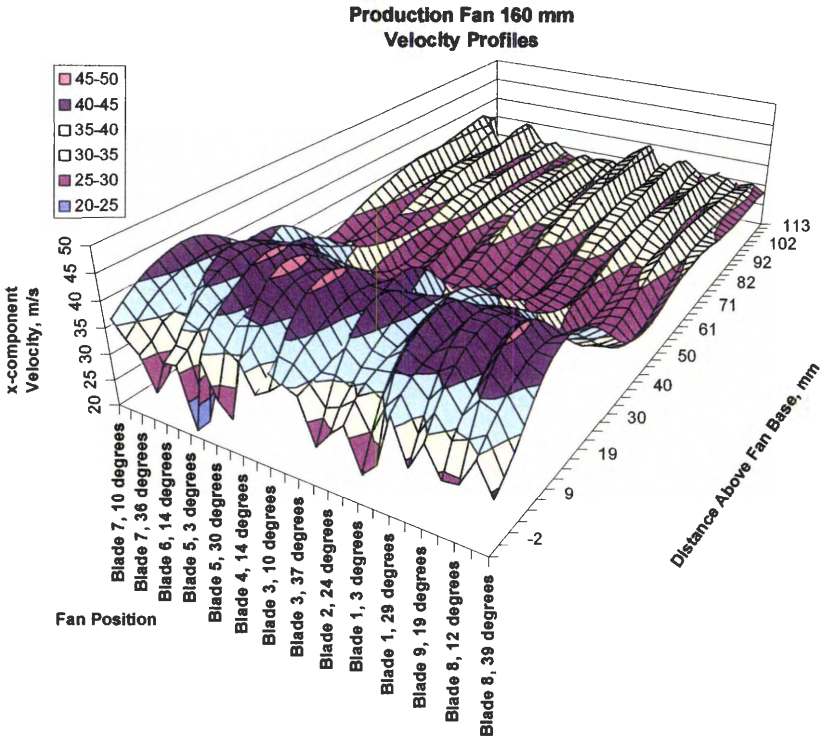

Figure 4.19 Surface contours of Production Fan Velocity Profiles Over One Fan Cycle: (a) 120 mm, (b) 160 mm offset from fan shaft

a

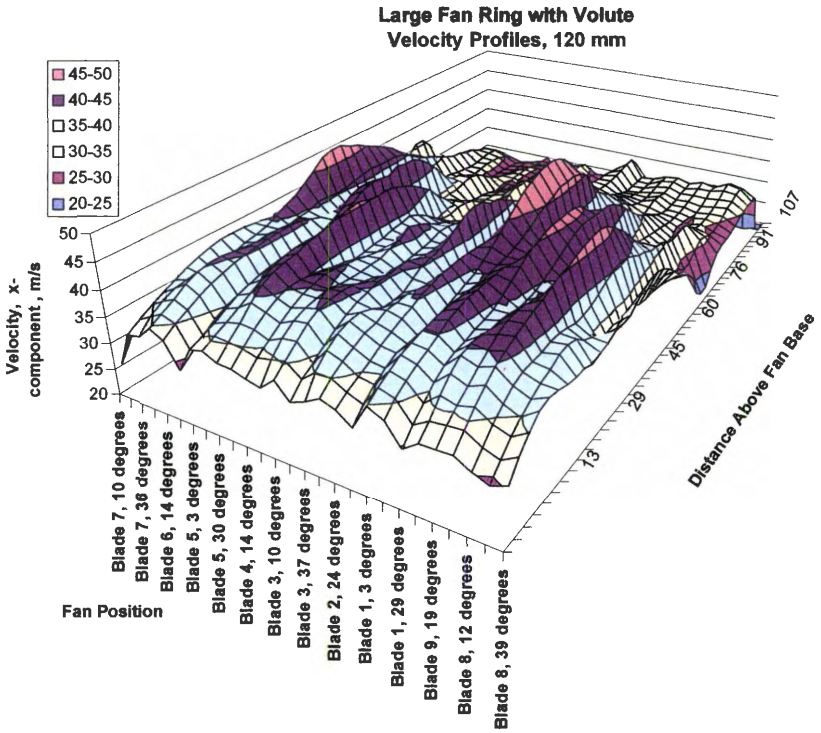

b

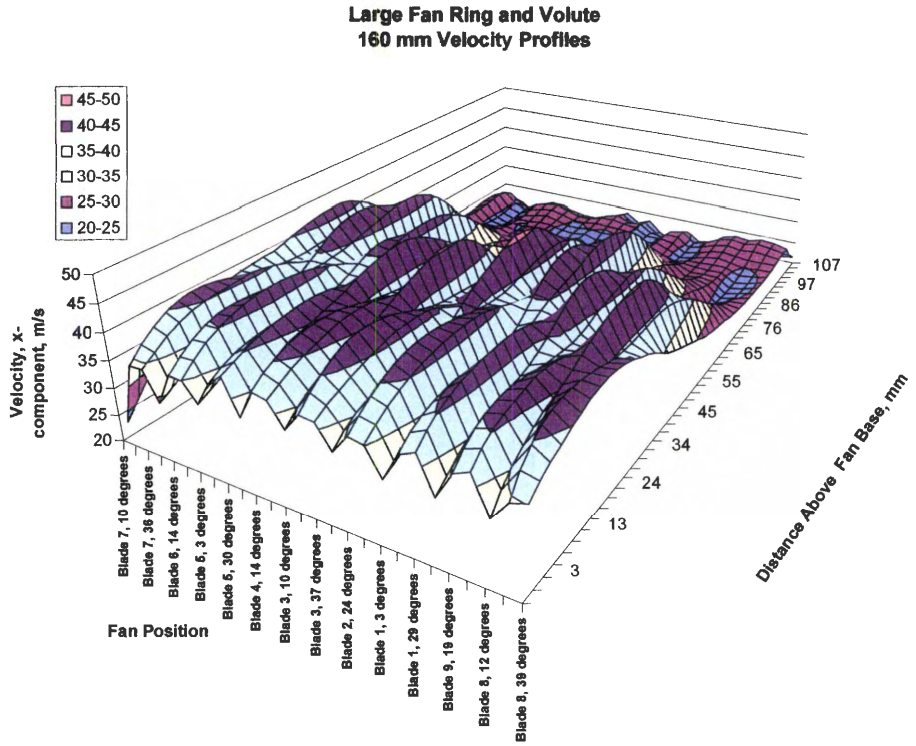

Figure 4.20 Surface contours of Fan with Large Ring Velocity Profiles Over One Fan Cycle: (a) 120 mm, (b) 160 mm offset from fan shaft

These plots also do not show a velocity decrease near the middle of the vector field. Velocity does decline near the top of the blower housing but is generally more uniform than with the production fan. Thus, the addition of the fan ring appears to generate greater uniformity of the flow and can be expected to result in less noise than the production fan without the ring.

Figures 4.21 (a) and (b) are surface contour plots of x-component air velocity for both the production fan and the fan with large ring at a 160 mm offset from the fan shaft shown in a top view which causes them to appear as two-dimensional contour plots. The red lines superimposed on the plots indicate the passage of fan blades. This facilitates viewing of the velocity profiles relative to each of the blade passings.

Regions of higher velocity air movement are in good agreement with the passing of each blade on both plots. That is, there is little difference in velocity profiles associated with the passage of the different blades. This suggests that the effect of varying intervals between blade passages appears minimal for the production fan. For the production fan the 47.5-50 m/sec velocity band rises to 70 mm from the fan base through the fan cycle. The fan with large ring and volute combination shows more variation; the 47.5-50 m/sec velocity band reaches between 70 to 90 mm from the fan base up into the blower housing as each fan blade passes in turn. The higher velocity areas follow the wider blade spacing by approximately 30 degrees.

This increased variability with the fan with large ring could be expected to result in more noise; however, as was previously noted, this fan was found to be quieter than the production fan. The complexity of this system as well as the need for caution in making inferences from a single plane of PIV data is emphasized.

a

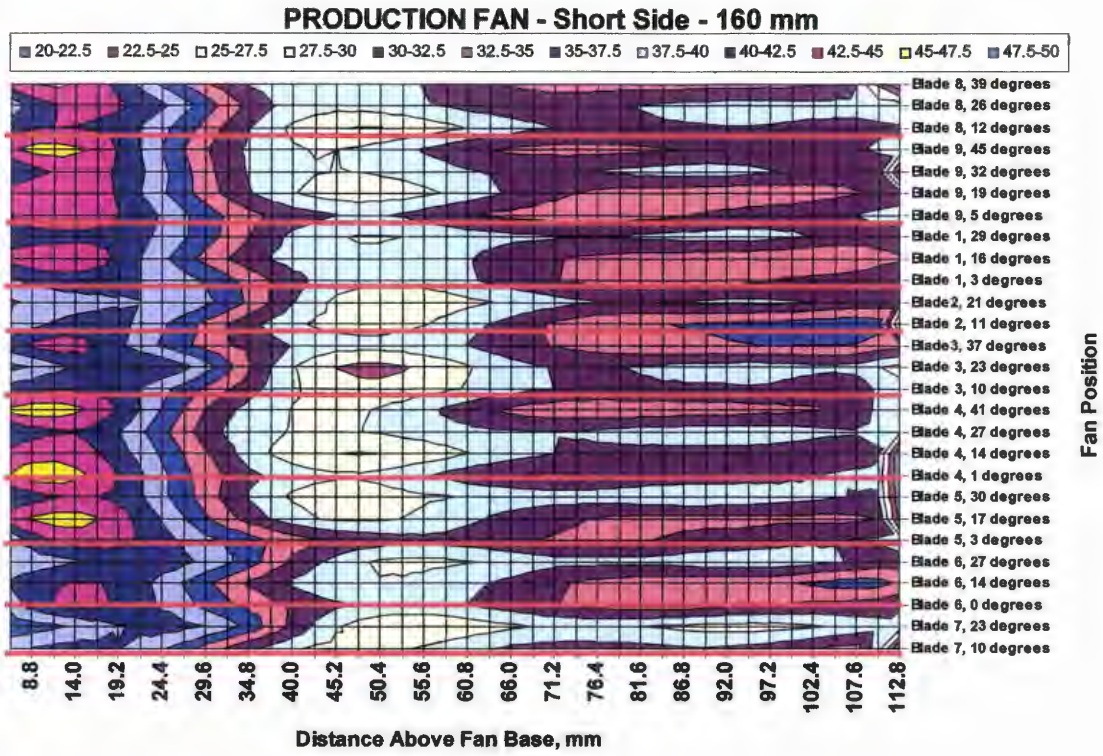

b

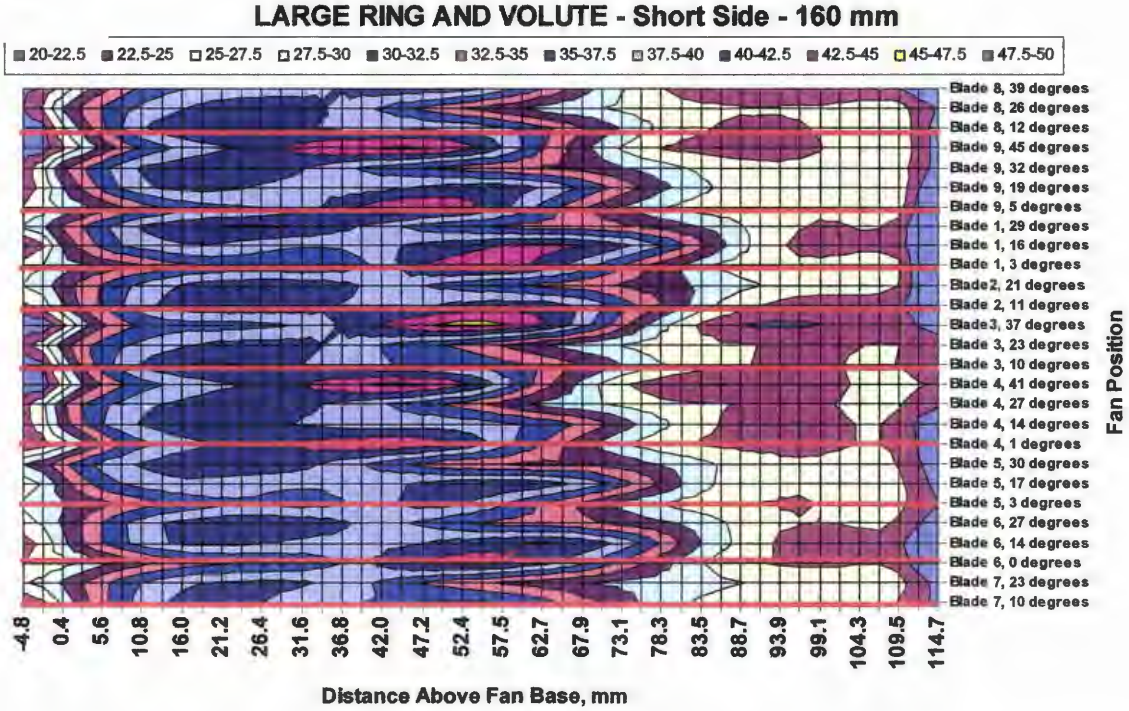

Figure 4.21: (a.) Production Fan, Contour Plot with Fan Blade Positions marked, (b.) Fan with Large Ring and Volute with Fan Blade Positions Marked

4.4 PIV Measurements in Five Horizontal Planes

The flow on the left hand side of the blower housing close to the fan and near the blower housing wall was not visible using the blower housings modified for the initial experiments. Windows built to follow the exact contours of the blower housing in that area would have resulted in considerable distortion of the PIV images due to the curved surfaces, and furthermore, they would have been very difficult to fabricate. In an effort to obtain data in this area, a blower housing was equipped with flat windows as shown in Fig. 2.7. The contours of the blower housing were changed slightly from the actual production contours by this modification; however it was expected that PIV observations on planes well away from the altered curvature would be minimally influenced.

Ensembles of 1000 images were collected on horizontal planes 20, 40, 60, 80, and 100 mm above the fan base. The PIV system was set to self trigger for these observations resulting in observations at random fan positions. The vector fields obtained from the PIV images were ensemble-averaged to produce a vector field showing the mean flow on these planes independent of fan blade position. Observations were made using the production fan, the fan with large ring and the production fan with an experimental volute insert installed.

Figure 4.22 contains the vector fields produced from these observations. The first column in this figure shows the five vector fields obtained using the production fan. The streamlines plotted with the vector field show the flow parting against the blower housing wall with part of the flow being diverted back into the fan. This recirculation is occurring on all levels observed using this fan.

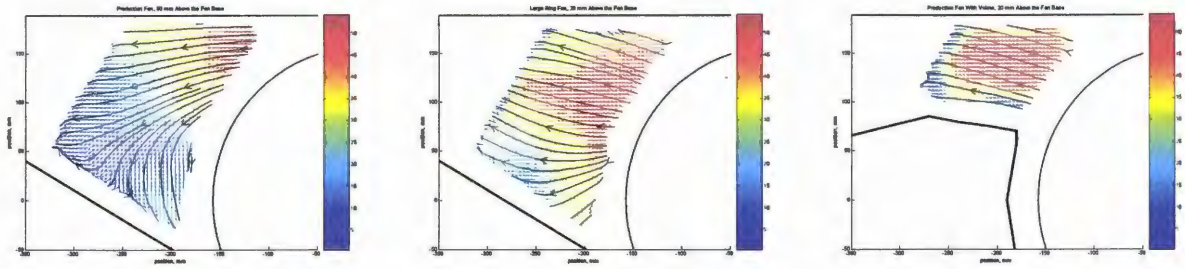

20 mm

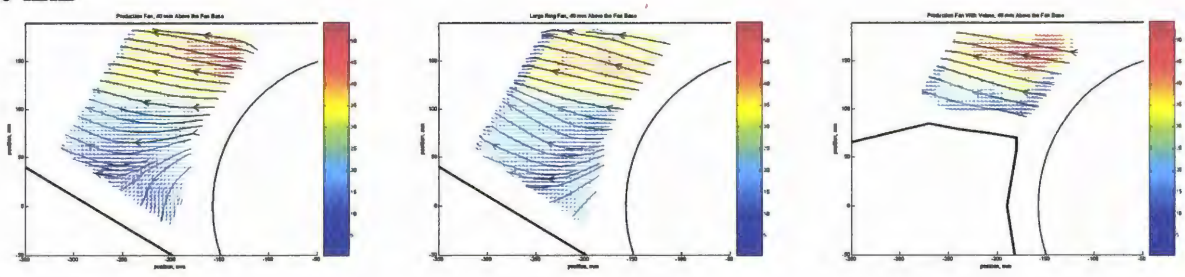

40 mm

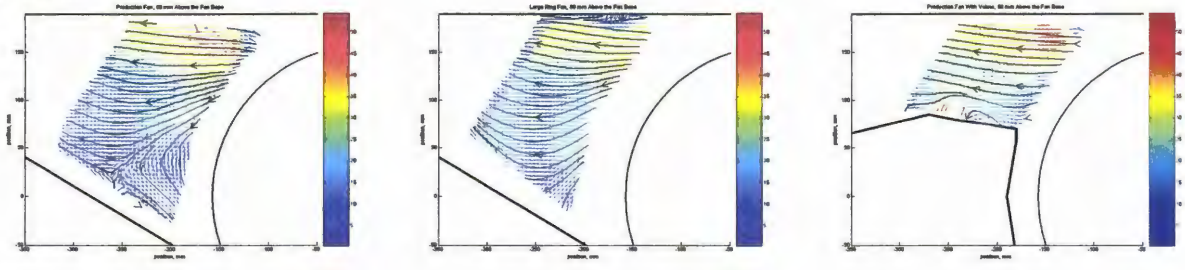

60 mm

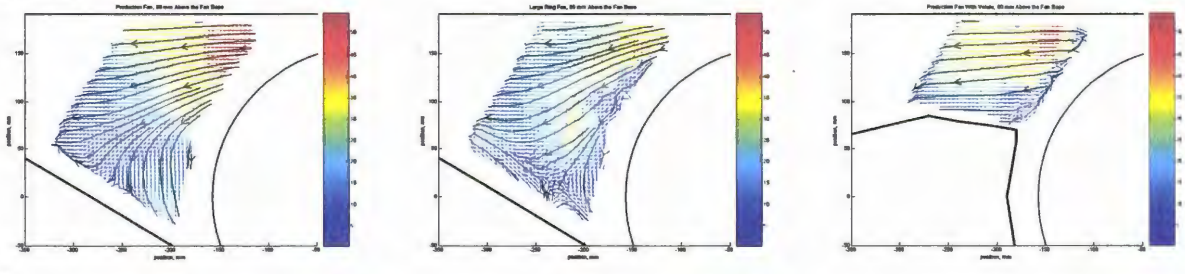

80 mm

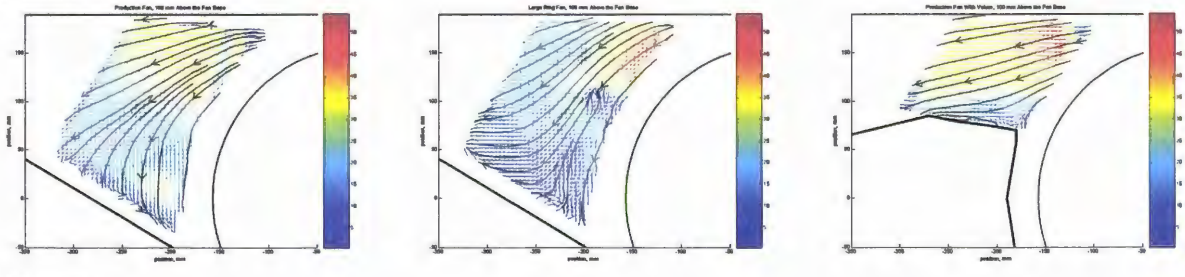

100 mm

Figure 4.22 Averaged Vector Fields; Horizontal Planes, First Column, Production Fan; Second Column, Fan with Large Ring; Third Column, Production Fan with

The second column of vector fields was produced using the fan with large ring. With this configuration recirculation is evident at the 80 and 100 mm levels and is beginning at the 60 mm level.

The third column of vector fields was produced using the production fan with a volute added to the blower housing on the left hand side.

It was hypothesized that the air seen reentering the fan was reducing the fan's operating efficiency and increasing the noise produced. This suggested that the region in the blower housing where air was observed returning to the fan could be filled in since air movement there was not contributing to the desired flow. This would retain air in the fan longer and increase flow on the opposite (right hand side of the blower housing), also increased efficiency should reduce noise produced. A volute was constructed to test this hypothesis. This volute was shaped to fill in the area where recirculation was observed, matched to observations on each level where PIV measurements were made.

This change did prevent the recirculation that had been previously observed. However testing showed a 15% decrease in flow with the volute installed. This flow reduction may have been due to the particular volute shape chosen acting as an obstruction to the exit flow. Also noise production was increased by approximately 1 dbA. The increased noise production is consistent with findings of Velarde-Suarez *et al.* (1992) which state that interaction of a centrifugal fan impeller with the volute tongue is a major cause of pressure fluctuations which can result in noise. The simulation they used predicted increased noise as the distance between impeller and volute tongue decreased. The blower housing modification which directed air out of the blower housing rather than allowing reingestion by the fan placed a volute tongue where none had existed before. These results highlight the

interdependence of system components which can cause difficulty in finding changes which improve performance.

5 CONCLUSIONS AND RECOMMENDATIONS

To the authors knowledge this was the first attempt to collect PIV data in a commercially produced blower housing. Modifications to the test stand and blower housing were necessary to allow optical access. A shaft encoder was added to the test stand to enable the collecting of images at a specified point in the fan cycle.

Data was first collected on three vertical planes (planes parallel to the fan's axis) in both the left and right hand side of the blower housing. These measurements were done for three fan positions during the passage of one fan blade using the production fan and blower housing with no modifications. The motivation for these measurements was to establish the feasibility of collecting PIV data in this blower housing, test the operation of the fan shaft encoder, and to gain knowledge of the system's flow characteristics to assist in designing further investigations. The flow was found to pulse with the passage of the fan blades. Higher velocity flow was seen near the bottom of the blower housing (base of the fan). This was indicative of a fan operating under significant restriction.

For the next set of measurements undertaken, three different prototype fans were provided by the Bobcat Corporation. These fans differed from the production fan in that part of each blade was cut away at the top inside corner and a proprietary modification was made to the fan's base geometry. Two of the fans were equipped with rings attached to the outside top of the blade to guide air from the fan's axial direction to the radial direction into the blower housing. The rings were of two different sizes to test the effect of differing geometry. These measurements were performed for five fan positions over the passage of one fan blade. Measurements were made on vertical and horizontal planes located near the center of the blower housing for this series of experiments. In addition to the three fan configurations

tested, a volute insert was produced which could be installed on the left side of the blower housing to give it the same fan cutoff geometry as that found on the right hand side.

The fan without a ring produced a flow similar to the standard production fan with higher velocity flow low in the blower housing. With the volute insert installed the velocity was more uniform along the depth of the fan. However, noise increased due to the volutes interaction with the fan, resulting in a 1 dbA overall sound power increase. The fans equipped with rings produced more uniform flow both with and without the volute insert. Higher velocity flow was seen near the bottom of the blower housing with a lesser area of high velocity near the top. The areas of differing velocity are suspected as regions where noise may be produced from turbulence generated by shear in the flow. Not all situations with differing velocities had higher noise levels however, which highlights the difficulty in making predictions with only one plane of PIV data. The larger fan ring produced the quietest flow. The smaller fan ring may have produced more noise due to its smaller radius resulting in flow separation with accompanying turbulence. Addition of the volute insert caused a substantial increase in sound power output with all fans tested. The literature strongly suggests that this noise increase is due to fan/volute tongue interaction.

The relative performance of all the fan blades was investigated by dividing one turn of the fan into twenty-seven equal intervals and taking data at each corresponding fan position. The production fan and fan with large ring and volute installed were tested in this manner. The data were grouped according to the angle of the blade from the PIV plane. Velocity profiles from the vector fields obtained at each of the twenty-seven positions were compared to each other in groups within 5 degrees of each other. The individual blades were determined to be performing similarly with only minor deviations. The production fan

produced a higher velocity flow at the bottom of the blower housing as was previously observed. The fan with large ring and volute produced a more uniform flow with higher velocities near the center of the fan.

Flow in the area of the blower housing where no volute cutoff was present was investigated by collecting data on five horizontal planes 20, 40, 60, 80 and 100 mm above the fan base. Data were obtained at random points of the fan cycle by setting the PIV system to obtain images at its own cycling rate rather than externally triggered by the shaft encoder. One thousand vector fields were averaged for each of the five levels. The vector fields thus obtained show reentry of air into the fan at all levels with the production fan and at the higher levels with the fan with large ring. A volute was made to fill in the area where flow was being reingested by the fan based on the PIV information. The reentry of air to the fan was eliminated by this volute. However noise was again increased and flow was adversely affected. Further work in developing the volute shape could eliminate the reduction in flow. Another option could be to eliminate the cutoff on the right hand side of the blower housing, since this could result in noise reduction.

Further study of this air handling system should include the intake area of the fan. This could be done using PIV or a multi-hole probe to obtain directional information. The multi-hole probe would be more intrusive than PIV and yields data one point at a time, but initial costs are lower and optical access is not needed. Likewise the area near the fan where reingestion of the flow was found could be investigated. The flow is highly three-dimensional so the out of plane flow not seen in the present PIV work is of interest. Here again a multi-hole probe could be useful as well as PIV data in different planar orientations.

Study of flow near the volute tongue could suggest ways to obtain the benefits of including a volute in the blower housing design without incurring the noise penalty.

Finally, the PIV data from this and possible future studies could be used to aid in the development of CFD models of centrifugal fan flows in blower housing assemblies. Once developed, these CFD models could be of great utility in the design process, since design changes could be tested using a computer instead of a time consuming trial-and-error procedure involving experiments on successive prototypes.

REFERENCES

ANSI S12.36-1990 (R 1997) American National Standard Survey Methods for the Determination of Sound Power Levels of Noise Sources, 1997

Chu, S; Dong, R.; Katz J.,"Relationship between unsteady flow, pressure fluctuations, and noise in a centrifugal pump-Part A: Use of PDV data to compute the pressure field", *ASME Journal of Fluids Engineering*, Vol. 117, pp. 24-29, 1995.

Chu, S; Dong, R.; Katz J.,"Relationship between unsteady flow, pressure fluctuations, and noise in a centrifugal pump-Part B: Effects of blade-tongue interactions", *ASME Journal of Fluids Engineering*, Vol. 117, pp. 30-35, 1995.

Fehse, K., Neise, W., 1998, "Generation Mechanisms of Low-Frequency Centrifugal Fan Noise" AIAA/CEAS Aeroacoustics Conference, 4th (19th AIAA Aeroacoustics Conference), Toulouse, France; UNITED STATES; 2-4 June 1998. pp. 948-958.

Feng, Hua ;Olsen, Michael G.; Liu, Ling; Fox, Rodney O.; Hill, Janes C., " *Investigation of Turbulent Mixing in a Confined Planar Jet Reactor*", AIChE Journal, Vol. 51, No. 10, pp. 2649-2664, October 2005.

Hamkins, C. P., and Flack, R. D., ''Laser Velocimeter Measurements in Shrouded and Unshrouded Radial Flow Pump Impellers'' *ASME J. Turbomachinery*, 109, pp. 70–76, 1987.

Lee, Gong Hee; Baek,Je Hyun; Myung, Hwan Joo, "Structure of Tip Leakage Flow in a Forward-Swept Axial-Flow Fan", *Flow Turbulence and Combustion* 70: 241-265, 2003.

Meakhail, T, Park, S.," A Study of Impeller-Diffuser-Volute Interaction in a Centrifugal Fan",*ASME Journal of Turbomachinery,* Vol. 127 pp.84-90, 2005.

Meakhail, T., Zhang, L., Du, Z. H., Chen, H. P., and Jansen, W.,''The Application of PIV in the Study of Impeller Diffuser Interaction in Centrifugal Fan. Part I—Impeller-Vaneless Diffuser Interaction,'' Proceedings of The ASME Fluid Engineering Division-IMECE2001/FED-24952 November 11–16, 2001, New York, USA.

Meakhail, T., Zhang, L., Du, Z. H., Chen, H. P., and Jansen, W.,''The Application of PIV in the Study of Impeller Diffuser Interaction in Centrifugal Fan. Part II—Impeller-Vaned Diffuser Interaction,'' Proceedings of The ASME Fluid Engineering Division- IMECE2001/FED-24953 November 11–16, 2001, New York, USA.

Olsen, M. G., "Private Communication", September 2005.

Paone, N., Riethmuller, M. L., and Van den Braembussche, R. A., ''Experimental Investigation of the Flow in the Vaneless Diffuser of a Centrifugal Pump by Particle Image Displacement Velocimetry'' *Experiments in Fluids*, 7, pp. 371–378, 1989.

Prasad, A.K., Adrian, R. J., Landreth, C.C., and Offut, P.W.,"Effect of resolution on the speed and accuracy of particle image velocimetry" *Experiments in Fluids,* 13, pp. 105-116, 1992

Shepherd, I.C., Lafontaine. R.F., "Measurement of vorticity noise sources in a centrifugal fan", *Proc. FAN NOISE Symp.,* pp. 205 212, Senlis, Francia, 1992

Velarde-Suarez, S.; Ruiz-Fuertes, P.; Ballesteros-Tajadura, R.; Santolaria-Morros, C., 2000, "Pressure Fluctuations and Generation of Tonal Noise in a Centrifugal Fan", In Proceedings of 9th International Symposium on Unsteady Aerodynamics, Aeroacoustics and Aeroelasticity of Turbomachines (ISUAAAT) and Legendre Lecture Series, Lyon, France, Sept. 4-8, 2000. pp. 160-169.

White, Frank M., "Viscous Fluid Flow *Second Edition*", McGraw Hill, Inc, Pages 163-168, 1991.

Yoon, Jong-Hwan, Lee, Sang-Joon, "Stereoscopic PIV measurements of flow behind an isolated low-speed axial-fan", *Experimental Thermal and Fluid Science* Volume 28, Issue 8, Pages 791-802, 2004.

.